# Matrix Isolation of Ions and Ion Pairs

Using Pulsed Laser Deposition of Non-Volatile Halides and Pseudohalides

Inaugural-Dissertation
to obtain the academic degree
Doctor rerum naturalium (Dr. rer. nat.)

submitted to the
Department of Biology, Chemistry and Pharmacy
of Freie Universität Berlin

by

Frenio A. Redeker

December 2019

The work for this dissertation was done in the time period from August 2016 to December 2019 under the supervision of Prof. Dr. Sebastian Hasenstab-Riedel at the Institute of Chemistry and Biochemistry of Freie Universität Berlin.

| | |
|---|---|
| 1st Referee: | Prof. Dr. Sebastian Hasenstab-Riedel |
| 2nd Referee: | Prof. Dr. Kevin Pagel |
| Date of Defense: | 28.02.2020 |

# Acknowledgements

First of all, I would like to thank my supervisor, Prof. Dr. Sebastian Hasenstab-Riedel, for giving me the opportunity to conduct my doctoral work in his lab on a satisfying topic, for his continuous support, for his contagious enthusiasm and motivation, and for the degree of freedom he gave to me.
I would like to thank Prof. Dr. Kevin Pagel for his time and effort to assess my work as a second reviewer.
Thanks also to the other members of my examination commission for their time and effort.
I am especially grateful to my mentor, Dr. habil. Helmut Beckers, for proofreading all my manuscripts and giving me valuable feedback, for always being approachable, for inspiring scientific discussions, for his continuous guidance and invaluable advice.
Thanks to Prof. Dr. Mingfei Zhou for giving me the opportunity to visit his laboratory at the Fudan University in Shanghai and to Guohai Deng, Dr. Jiaye Jin, and Qian Wang for their companionship during my stay.
Thanks to Prof. Dr. Lester S. Andrews for fruitful and delightful conversations, for valuable advice, and for welcoming me to a brief visit to Charottesville, Virginia this summer.
I am very grateful to Dr. Simon Steinhauer, Dr. Carsten Müller, Dr. Günther Thiele and Dr. Moritz Malischewski for their scientific advice.
Thanks to Alexey Kropman (Bachelor's thesis and internship) and Patrick Voßnacker (internship) for their help and their motivation while working under my supervision.
I am especially thankful to all members of the Riedel lab for providing a lovely work environment, for fruitful discussions and for everyone's willingness to help with all kinds of problems in the day-to-day business. I had a great time working with you all.
Thanks also to the staff of the Materialverwaltung, the technical staff, the glass blowers, the workshops of the chemical and the physical department and to the whole staff of the inorganic department.
I would like to thank the Zentraleinrichtung für Datenverarbeitung (ZEDAT) for computing resources and support.
Thanks to all my friends and family for their kindness and support, for bringing me joy and for their generosity to forgive my occasional failure to take care of our relationship to the extent it deserves. Thanks for having me in your lives.
Finally, I would like to thank my dear parents, Beate and Franz Redeker, my dear brother, Markus Gramenz, and my beloved partner, Helen Toner. Thanks for all the support and encouragement I receive from you.

# Matrix Isolation of Ions and Ion Pairs

Using Pulsed Laser Deposition of Non-Volatile Halides and Pseudohalides

Frenio A. Redeker

**Abstract:** The vaporization of high melting compounds for matrix-isolation spectroscopic investigations has always been a challenging experimental endeavor. Here, pulsed laser deposition is used to vaporize non-volatile halides and pseudohalides for subsequent co-deposition of the ablation products with an excess of matrix gases. This method is shown to yield good results in a fraction of the time compared to Knudsen effusion and, more importantly, allows for the isolation of free anions. Pulsed laser deposition of alkali fluorides and chlorides (MF and MCl, M = Li-Cs) and their co-deposition with dihalogen ($F_2$ and $Cl_2$) led to the observation of new vibrational bands of free $F_3^-$ and some alkali ion pairs ($MF_3$ and $MCl_3$) in solid neon and the first observation of free $Cl_3^-$. Matrix isolation of laser ablation products of the pseudohalide KCN yielded, among a variety of polycarbon and polynitrogen compounds, the novel ion pairs $KC_3$ and $KN_3$. Molecular potassium azide ($KN_3$) was shown to exist as a side-on and an end-on isomer. As a further developement of the plain salt ablation, it was possible to investigate molecular alkali ion pairs of the tetrafluorido aurate ($AuF_4^-$) by co-deposition of laser-ablated $MF/AuF_3$ mixtures in solid neon matrices. All results were validated by high-level quantum-chemical calculations and are here presented in the context of the present state of research.

**Zusammenfassung:** Das Verdampfen schwerflüchtiger Substanzen für matrix-isolationsspektroskopische Untersuchungen war und ist eine Herausforderung für Experimentatoren. Im Rahmen der vorliegenden Arbeit wurde die Methode der Laser-Ablation für die Verdampfung von schwerflüchtigen Halogeniden und Pseudohalogeniden für die Anwendung in der Matrixisolationsspektroskopie untersucht. Diese Methode der Verdampfung liefert nicht nur gute Ergebnisse in einem Bruchteil der Zeit verglichen mit herkömmlichen Hochtemperaturmethoden, sondern führt auch zur Ionisation der verdampften Salze. So konnten durch Abscheidung laser-ablatierter Alkalifluoride und -chloride (MF und MCl, M = Li-Cs) mit den Dihalogenen $F_2$ und $Cl_2$ neue Schwingungsbanden für freies $F_3^-$ und einige Alkali-Ionenpaare ($MF_3$ und $MCl_3$) in Neon-Matritzen erhalten und freies $Cl_3^-$ erstmals IR-spektroskopisch beschrieben werden. Durch Isolation der Ablationsprodukte des Pseudohalogenids KCN war es außerdem möglich, neben einigen Polykohlenstoff- und Polystickstoffverbindungen, die neuartigen Ionenpaare $KC_3$ und $KN_3$ zu isolieren. Molekulares Kaliumazid ($KN_3$) konnte dabei sowohl als end-on-, als auch als side-on-Komplex nachgewiesen werden. Durch Weiterentwicklung der reinen Salzablation konnten Alkali-Ionenpaare des Tetrafluoridoaurats ($AuF_4^-$) durch Abscheidung laser-ablatierter $MF/AuF_3$-Mischungen in Neon-Matritzen erzeugt und charakterisiert werden. Alle Ergebnisse sind mithilfe quantenchemischer Rechnungen abgesichert worden und werden hier im Kontext früherer Arbeiten präsentiert.

# List of Abbreviations

| | |
|---|---|
| 3c-4e | 3-center 4-electron |
| B3LYP | Becke 3-parameter Lee-Yang-Parr |
| BP86 | Becke 1988 and Perdew 1986 |
| CASSCF | complete active space self consistent field |
| CC | coupled cluster |
| CCSD(T) | coupled cluster singles, doubles and pertubational triples |
| DFT | density functional theory |
| EPR | electron paramagnetic resonance |
| ESP | electrostatic potential |
| FIR | far infrared |
| FTIR | Fourier transform infrared |
| HF | Hartree-Fock |
| HOMO | highest occupied molecular orbital |
| IR | infrared |
| ISC | intersystem crossing |
| LUMO | lowest unoccupied molecular orbital |
| MCT | mercury cadmium telluride |
| MP2 | second-order Møller Plesset perturbation theory |
| MRCI | multi reference configuration interaction |
| Nd:YAG | neodynium-doped yttrium aluminum garnet |
| NPA | natural population analysis |

| | |
|---|---|
| PLD | pulsed laser deposition |
| PXRD | powder X-ray diffraction |
| SCS | spin-component scaling |
| SI | Supporting Information |
| SOMO | singly occupied molecular orbital |
| STE | self trapped exciton |
| UV | ultraviolet |
| UV/Vis | ultraviolet and visible |
| XRD | X-ray diffraction |

# Contents

# 1 Introduction

Gaining insight into bond properties, reactivities and structures of chemical compounds is the mission of modern chemistry. Ideally it is possible to use such insight to investigate and develop new materials and chemical processes in a straightforward fashion and thereby establish a basis for technical progress. Knowledge of the ability of molecules to form chemical bonds and the characteristics of such bonds is the key requirement for making predictions about the formation and reactivity of new materials.

An important example of a chemical bond that is currently under intensive investigation is the halogen bond, which promises high importance for applications in the fields of electrochemistry, organic synthesis and ionic liquids, to name just a few.[1,2] Polyhalogen anions are especially promising candidates for the optimization of industrial processes, e. g. for the storage and purification of dihalogens,[3] since polyhalogen anions can consume or release dihalogen molecules depending on the conditions. Ionic liquids with polychlorine anions, have recently been shown to serve as efficient oxidants to selectively dissolve $UO_2$ from a mixture with lanthanides[4] and might therefore find applications for the purification of rare earth metals.

In order to study the nature of a certain chemical bond it is important to reduce competing interactions to a minimum, which can be achieved by either studying the molecules involved in the gas phase or by isolation of the system in a weakly interacting medium, e. g. a rare gas matrix. The latter approach was used in this thesis work and will be discussed in more detail in the following section.

## 1.1 The Matrix-Isolation Technique

A powerful method to investigate molecules in a weakly interacting medium is the matrix-isolation technique developed by George C. Pimentel in the 1950s. In combination with various spectroscopic methods and quantum-chemical calculations matrix isolation allows for the thorough characterization of molecules and can yield valuable information about the bonding properties and the reaction behavior of the isolated molecules. Results obtained by matrix-isolation spectroscopy also serve as important benchmarks for the evaluation of the methods used in theoretical chemistry as the molecules are studied under pseudo gas-phase conditions at very low temperatures where only electronic and vibrational ground states are populated (an exception might be $UO_2$ in solid argon[5]) and rotational transitions are suppressed (except for a few small molecules like $H_2O$[6]) which makes the spectra obtained

from matrix isolated species easy to interpret in the ideal case.

Compounds in the liquid or solid phase are involved in intermolecular interactions which influence and potentially change the properties of the intramolecular bonds. The structure of a trichlorine anion ($Cl_3^-$) in a crystal, for example, will depend on interactions with the surrounding counter cations. Thus, the bond lengths of the anion will change with different cations. There are two possibilities to study an isolated trichlorine anion: either in the gas phase or by matrix-isolation. The low temperatures at close to absolute zero (3-20 K) used for matrix isolation also strongly reduce reaction rates, e. g. for monomolecular rearrangement reactions, and thereby allow for the investigation of highly reactive intermediates.

In a typical matrix-isolation experiment precursors of the reactive species that are to be investigated are co-deposited on a matrix support with an excess of an inert gas at 3-20 K, depending on the host gas. The rare gases Ne and Ar are most commonly used as host gases, but Kr, Xe, $N_2$, $CO_2$, $H_2$, $CH_4$, adamantane, alkanes and perfluorinated alkanes can also be used. Even pure $F_2$ can be used as a reactive matrix host[7] in order to stabilize elements in high oxidation states. Neon is the most suitable host gas as measured by its low interaction with guest molecules and the transparency of the matrix. The main disadvantage of neon is that its matrices cannot be annealed above a maximum of 13 K at which sublimation occurs. For comparison, argon matrices can be annealed to above 30 K, krypton matrices to above 40 K, xenon matrices even higher. However, interactions with the guest material increase in the same direction so that some elusive molecules are only observed in solid neon.

Aim of the matrix-isolation method is to isolate single molecules of the guest compound and to reduce di-, tri- and oligomerization to a minimum. In the combination of matrix isolation and pulsed laser deposition the occurrence of one molecule or atom of the laser ablated material with one molecule of the reactive gas in the same cavity is desired. Probably the most common spectroscopic method used in combination with the matrix isolation technique is infrared (IR) spectroscopy. However, Raman,[8] ultraviolet and visible (UV/Vis),[9] and electron paramagnetic resonance (EPR) spectroscopy[10,11] are commonly used as well. Ideally the isolation conditions lead to sharp bands in the IR spectra obtained after matrix isolation. Site bands, however, which occur from isolated guest molecules in different orientations, are a common phenomenon.

Any molecule that is volatile enough to be vaporized without decomposition can be used as a matrix guest. If the guest substance is a gas, it can be mixed with the host gas in an arbitrary concentration prior to the deposition. If the guest is a volatile liquid or solid, it can be filled into a u-tube with a bypass. The host gas is then guided through both the bypass and the u-tube during deposition. The concentration of the guest in the deposit can be controlled by adjusting the vapor pressure of the guest substance through heating or cooling depending on the experimental demands. Solids with low volatility can be vaporized in a Knudsen cell, consisting of a quartz (or other) tube and a heating filament, through which the matrix gas is guided to carry the guest molecules in the gas phase to the matrix support. Thermal decomposition products of precursor molecules can be studied in a controlled

way by mounting a heated quartz tube in front of the matrix chamber through which the host/precursor-mixture is directed prior to deposition. Radicals and charged species of gaseous precursors can be produced by co-deposition of host/precursor-mixtures with host atoms from a microwave discharge. A powerful method for the vaporization of high-melting compounds, the laser-ablation technique, is discussed in detail in the following section.

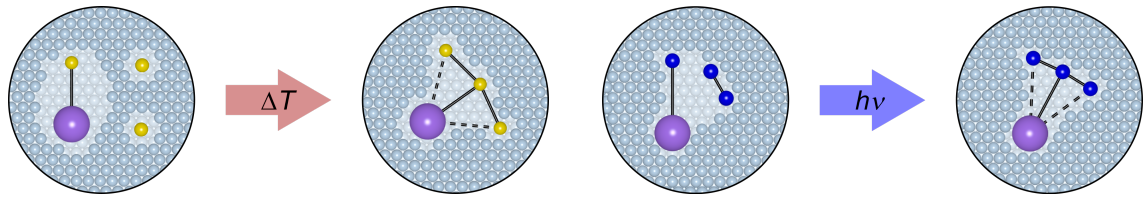


**(a)** Formation of $KF_3$. **(b)** Formation of $KN_3$.

**Figure 1.1:** (a) A reaction that is enabled by diffusion of molecules during annealing, (b) a photochemical reaction that is triggered by irradiation.

Figure 1.1 shows an illustration of an annealing and an irradiation experiment, which are two important methods to gather information about matrix-isolated molecules. The word annealing describes the heating of the matrix to a certain temperature. After that temperature has been reached, the matrix is usually cooled to the deposition temperature before the next spectrum is measured. Figure 1.1a shows the formation of potassium trifluoride ($KF_3$) in a neon matrix by diffusion fluorine atoms triggered by annealing. First, KF and two F atoms are isolated in separated cavities. Annealing allows for the diffusion of fluorine atoms and a reorientation of KF. Once KF and the F atoms are in the same cavity they react to yield $KF_3$. In contrast to atoms, molecules cannot travel within the matrix during annealing. Figure 1.1b shows the formation of potassium azide ($KN_3$) by the reaction of potassium nitrene (KN) with dinitrogen ($N_2$). Although KN and $N_2$ are isolated in the same cavity, it is not possible for them to react. Photo excitation of the KN molecule is necessary to enable the reaction with $N_2$ to form $KN_3$. Based on their annealing and irradiation behavior it may sometimes be possible to assign a group of IR bands to the same molecular species, since some species are only formed by annealing or irradiation while others decompose and some remain unaffected.

Varying the concentration of the reactive gas is a suitable method to examine how many molecules of the reactive gas are involved in the formation of an isolated species. If the concentration of the reactive gas is decreased, bands belonging to product species that contain more molecules of the reactive gas should decrease in intensity compared to bands belonging to product species that contain fewer molecules of the reactive gas. For example, if $F^-$ reacts with $F_2$ in a matrix isolation experiment to yield $F_3^-$ and $F_5^-$, the ratio of the band intensities of $F_3^-$:$F_5^-$ should increase, if the $F_2$ concentration is decreased and vice versa.

Another very important tool for the assignment of IR bands obtained from matrix-isolation experiments is isotopic labeling. Mixed isotope experiments can provide valuable information about the number and type of atoms in a molecular species and about its molecular structure.

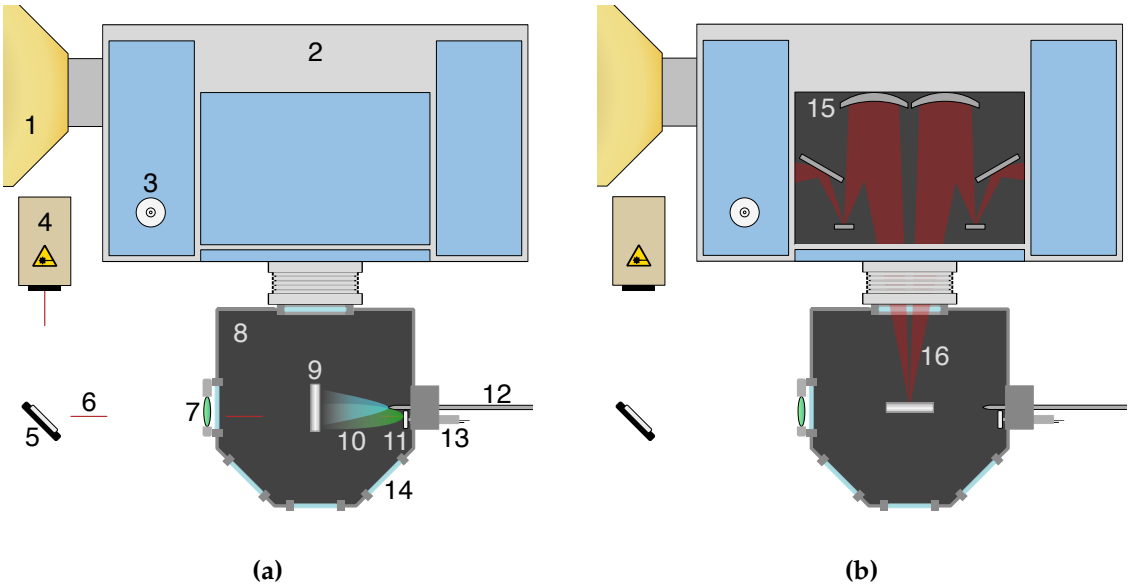


**Figure 1.2:** (a) Matrix-isolation setup illustrating the co-deposition of a laser ablated target material with a host gas at cryogenic conditions, (b) the same setup during measurement of an IR spectrum. 1 Helium cooled bolometer, 2 Fourier transform infrared (FTIR) vacuum spectrometer, 3 mercury cadmium telluride (MCT) detector, 4 neodynium-doped yttrium aluminum garnet (Nd:YAG) laser, 5 IR mirror, 6 laser pulse, 7 lense, 8 matrix chamber, 9 matrix support, 10 plasma plume, 11 target, 12 gas inlet, 13 target motor, 14 quartz window, 15 transfer optic, 16 IR beam.

A drawing of the matrix-isolation setup that was used in the course of this thesis is depicted in Figure 1.2. It shows a matrix chamber (8) that is kept at a vacuum of about $10^{-7}$ mbar by a rotary-vane pump followed by an oil diffusion pump. Turbo molecular pumps are more commonly used, but they are far more susceptible to corrosion than oil diffusion pumps. Therefore, an oil diffusion pump needs to be used when working with elemental fluorine and chlorine or other corrosive reactive gases. In the center of the chamber sits the rotatable matrix support (9). The matrix support, a gold plated copper block, can be cooled to 5-20 K using a cold head with a closed-cycle helium compressor unit. A heating cartridge near the matrix support allows for annealing of the matrix. It is also possible to use an IR transparent window, e. g. CsI as a matrix support for measurements in transmission. This would require the matrix chamber to be placed inside the spectrometer. For matrix-isolation EPR spectroscopy a thin copper rod could be used as a matrix support.[12] The target for laser ablation (11) is mounted on a rotatable target holder which is magnetically coupled to the target motor (13). IR and far infrared (FIR) spectra can be measured in reflection by rotating the matrix support about 90° via a transfer optic (15) using a vacuum FTIR spectrometer (2) equipped with a liquid helium cooled bolometer (1, 700-60 $cm^{-1}$) or a liquid nitrogen cooled MCT detector (3, 4000-350 $cm^{-1}$). Laser ablation is facilitated using a pulsed Nd:YAG laser (4) with a pulse length of 7 ns and a pulse energy of up to 50 mJ at a rate of 1-10 Hz.

The focused laser pulses reach the target through a hole in the matrix support. The matrix chamber has five windows (14). One CsI window that separates the matrix chamber from the spectrometer, a second window for IR laser pulses from the ablation laser and three further windows for irradiaion experiments and for the inspection of the matrix and the plasma plume during deposition. Two of the windows can be replaced by collimators with optical fibers in order to perform UV/Vis experiments.

## 1.2 Pulsed Laser Deposition

Pulsed laser deposition (PLD), also laser ablation[13], pulsed laser sputtering[12] or pulsed laser vaporization[14] can be used in combination with the matrix-isolation technique to vaporize high-melting compounds for subsequent co-deposition with a mixture of reactive and matrix gases. Figure 1.3 illustrates the series of events that occur during laser ablation using a pulsed nanosecond laser. Within femtoseconds, electrons are expelled from the target material leaving cationic material behind which is subsequently also expelled in a Coulomb explosion due to Coulomb repulsion. As the laser pulse further heats the target, thermal vaporization of target material occurs. At a certain temperature, a plasma is formed which completely absorbs the remaining pulse energy heating the plasma even further. A plasma that absorbs all light is called a black plasma. The scheme in Figure 1.3 is based on a personal communication by Prof. Jürgen Reif of the department of experimental physics and material science at the BTU Cottbus.

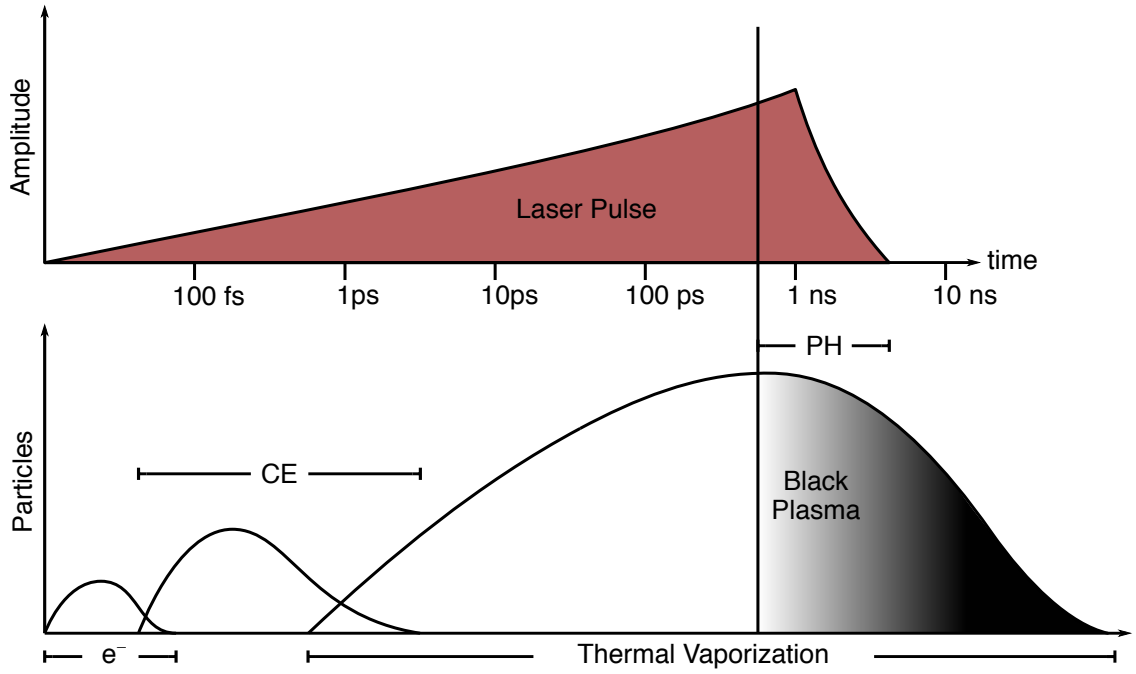


**Figure 1.3:** Qualitative depiction of the events happening during laser ablation when a laser pulse hits the target on a logarithmic time scale, CE (Coulomb explosion), PH (plasma heating).

Early papers that describe the use of laser ablation for matrix-isolation experiments state the difficulties associated with the vaporization of boron using conventional high temperature methods (Knudsen cell) as a reason to use an alternative method. The high melting point of boron, the high reactivity of molten boron and the resulting contaminants that are introduced from the vacuum system into the matrix due to the extreme heat are brought up as the main problems related to the conventional thermal vaporization techniques.[12,13] High-melting non-metals like boron[12,13] and carbon[15] were in fact among the first compounds to be studied using pulsed laser deposition in combination with matrix isolation. The use of pulsed and focused laser radiation to vaporize such compounds made it possible to avoid the problems related to conventional high temperature methods and had a useful side effect: since laser ablation leads to ionization of atoms in a plasma plume it is capable of producing charged species in addition to the neutral reaction products formed by thermal vaporization. Laser-ablation studies by Vladimir E. Bondybay showed that substantial amounts of atoms in metal vapors obtained from laser ablation are ionized.[14,16–18] In previous matrix-isolation studies, laser ablation has been most commonly used for the vaporization of pure non-metal and metal targets. There are also examples for the laser ablation of transition metal oxides[19] and high-melting main group compounds like boron nitride.[20] Matrix-isolation studies using laser ablation of element mixtures have been reported as well, but are rather exceptional, e. g. the CP radical has been reported in an EPR matrix-isolation study in 1988 and was produced by laser ablation of a mixed graphite and red phosphorus target.[10] Laser ablation of non-volatile alkali salts, however, can be considered a novelty to the field of matrix-isolation spectroscopy.

Considering that alkali halides are used as window materials for IR spectroscopy, it is not obvious or even counter intuitive that focused IR laser pulses can be used to vaporize such IR transparent materials. Table 1.1 shows the band gaps of the alkali fluorides and the number of photons needed for the multiphoton excitation of an electron to the conduction band using an Nd:YAG laser ($\lambda = 1064\,\mathrm{nm}$). The Nd:YAG laser used for laser ablation is operated at a pulse energy of about 50 mJ which amounts to $0.007\,\mathrm{J\,mm^{-2}}$ for a pulse diameter of 3 mm. The surface of a single CsF ion pair can be estimated using the ionic radii of 6-coordinate octahedral $Cs^+$ and $F^-$ and is $0.14\,\mathrm{nm^2}$. Using the unfocused laser beam, about 5250 photons would strike the area of one CsF ion pair during a 5 ns laser pulse. Assuming that a lens focuses the laser pulse by a factor of about $10^4$ to a beam diameter of 0.03 mm, it can be estimated that the ion pair is encountered by about 10 photons per femtosecond. This example calculation suggests that in principle multiphoton excitation can occur but is probably too rare to be the main driving force behind the laser ablation. Indeed, an experiment with a sodium fluoride single crystal showed little to no ablation of NaF and instead the aluminum target holder was damaged. Only targets of compressed powdery alkali halides are efficiently vaporized by IR laser ablation.

Crystal defects at the domain borders of the crystallites in the compressed pellet could play an important role in the laser ablation process since crystallographic imperfections

**Table 1.1:** Band gap energies of alkali fluorides and the number of photons ($\lambda = 1064\,\text{nm} = 1.165\,\text{eV}$) necessary for a multiphoton excitation.

| Material | Band Gap (eV) | Number of Photons | Reference |
|---|---|---|---|
| LiF | 13.6 | 12 | [21, 22] |
| NaF | 11.5 | 10 | [21, 22] |
| KF | 10.9 | 10 | [23, 24] |
| RbF | 10.4 | 9 | [23] |
| CsF | 10.0 | 9 | [23] |

lead to localized electronic states within the band gap and thereby enhance absorption of radiation.[25] It is further known that focused long-wavelength laser irradiation ($\lambda = 800\,\text{nm}$) can induce color centers in sodium chloride.[26] According to the book "Laser Ablation Mechanisms and Applications" by John C. Miller and Richard F. Haglund Jr. the process of laser ablation of alkali halides with an intense laser pulse of sub-bandgap energy can be described as follows: At the beginning of the laser pulse most photons penetrate through the bulk except for those involved in multi-photon band-to-band transitions. In the course of the laser pulse the top layers of the target become enriched with alkali metal while self trapped excitons (STEs) and color centers accumulate in the underlying regions. In the following, the underlying regions get also enriched with alkali metal and defects further improving absorption and leading to increasingly effective laser heating of the material at the later stages of a nanosecond laser pulse.[27]

**(a)** **(b)**

**Figure 1.4:** (a) Plasma plume during laser ablation of sodium fluoride, (b) caesium chloride target after laser ablation.

When compressed powder targets are used, the defect density at the domain borders between the crystallites is considered to be fairly high which should improve the absorption of focused IR laser radiation efficiently enough to explain the observed absorption behavior. Figure 1.4a shows the plasma plume during laser ablation of sodium fluoride (NaF). The color of the plasma resembles the characteristic flame color of sodium. Figure 1.4b shows the surface of a caesium chloride (CsCl) target after laser ablation. The deep grooves indicate

efficient ablation of material whereas the blue coloration is indicative for the formation of radiation induced color centers during laser ablation.

## 1.3 The Role of Computational Chemistry

Quantum-chemical methods are further important tools to validate assignments based on the results of matrix-isolation spectroscopic experiments. Most importantly, theoretical analysis of harmonic frequencies is used to facilitate interpretation of IR and Raman spectra of small molecules. Of the many programs available the TURBOMOLE[28] program package is especially useful for density functional theory (DFT) calculations. The MOLPRO[29] stack is well suited for all kinds of ab-initio calculations, while ORCA[30,31] is a solid program for DFT, second-order Møller Plesset perturbation theory (MP2), and coupled cluster (CC) calculations and emphasizes on the usability in combination with all kinds of spectroscopic methods.

DFT methods like Becke 3-parameter Lee-Yang-Parr (B3LYP)[32–35] and Becke 1988 and Perdew 1986 (BP86)[36,37] are usually used to validate vague guesses as these methods are computationally cheap and yield reasonable results for simple small molecules within minutes. If a higher accuracy is needed, the MP2 method can provide good results for small molecules in less than an hour. The MP2 method is commonly used with spin-component scaling (SCS) to improve the description of molecular ground state energies by separately scaling parallel- and antiparallel-spin components.[38] The coupled cluster singles, doubles and pertubational triples (CCSD(T)) procedure is the method that usually yields the most accurate results and the best agreement with experiments, however, it is also one of the most costly methods and only makes sense in combination with a basis set of triple zeta quality or higher. The calculation of a molecule consisting of four atoms with $C_s$ symmetry at the CCSD(T)/triple-$\zeta$ level, for example, will run for about a day on 8 parallel processors. The duration of a CCSD(T) calculation can quickly exceed weeks and months depending on the number of atoms and the symmetry of the molecule.

Where possible, IR spectroscopic results are validated using isotopically labeled experiments which usually allows for a clear structural assignment. However, some chemical elements have only one stable isotope such as the neat elements $^{19}F$ or $^{197}Au$. For matrix-isolation investigations of compounds that contain only mononuclidic elements like the polyfluorine anions ($F_n^-$) or gold fluorides ($Au_nF_m$), quantum-chemical calculations become especially important.

## 1.4 Trihalogen Anions and their Alkali Ion Pairs

The first evidence for the tendency of halogens to react with halides to form polyhalogen anions was reported in 1819 by Pierre-Joseph Pelletier and Joseph B. Caventou who produced strychnine triiodide by addition of iodine to strychnine.[39] Sophus M. Jørgensen is

considered the first author who published a systematic study on polyiodides by the reaction of metal iodides with $I_2$ (1870).[40] The first complete crystal structure determination of a triiodine salt ($NH_4I_3$) has been reported in 1935 by Rose C. L. Mooney.[41] Today more than 500 crystal structures containing triiodine anions ($I_3^-$) and higher polyiodine anions up to $I_{29}^{3-}$ are known.[42,43] The first tribromide ($Br_3^-$) and trichloride ($Cl_3^-$) and triinterhalide ($Cl_2Br^-$, $Br_2Cl^-$, $BrICl^-$, $I_2Br^-$, $Br_2I^-$, $I_2Cl^-$, etc.) compounds were described by Frederick D. Chattaway and George Hoyle in 1923.[44] For all heavier halogens (X = Cl, Br, I), higher polyhalogen monoanions and interhalogen monoanions are known. The largest and most recent examples are $I_{15}^-$,[45] $Br_{11}^-$,[46] $Cl_{13}^-$,[47] and $Cl(BrCl)_6^-$.[48] The developments in polyhalogen chemistry and halogen bonding have been summarized in several recent reviews.[1,2,42,43,49] The following sections will focus on previous investigations of trihalogen anions and ion pairs. Alkali ion pairs of $X_3^-$ anions will be written as $MX_3$ in the following. The notation $M^+X_3^-$ will occasionally be used if it serves clarity.

### The Trifluorine Anion

In the 1950s Hans Bode and Ernst Klesper postulated the synthesis of alkali trifluorides by reaction of alkali halides MX (M = K, Rb, Cs; X = Cl, Br, I) with a flow of elemental fluorine at 140-220 °C which they characterized via powder diffracton, density, and gravimetric measurements, claiming the formation of $MF_3$ either with the alkali metals in higher oxidation states or as ion pairs with a trifluorine monoanion ($M^+F_3^-$). They considered the latter possibility unlikely because extrapolation of the dissociation temperatures of $CsI_3$ (250 °C), $RbI_3$ (192 °C), $CsBr_3$ (148 °C), and $RbBr_3$ (106 °C) to the unknown salts $MCl_3$ and $MF_3$ led them to conclude that $M^+F_3^-$ could not be stable under their experimental conditions.[50,51] Later it became clear that the fluorine rich compounds Bode and Klesper had synthesized were in fact alkali tetrafluorido halates ($MXF_4$).[52,53]

The first undoubtful alkali trifluoride ion pairs $MF_3$ (M = Cs, Rb, K) were reported in 1976 by Bruce S. Ault and Lester Andrews who co-deposited thermally vaporized alkali fluorides (Knudsen cell) with difluorine ($F_2$) in solid argon under cryogenic conditions.[54,55] Ault and Andrews assigned a Raman band at 461 $cm^{-1}$ to the symmetric ($\nu_1$) and an IR band at 550 $cm^{-1}$ to the antisymmetric ($\nu_3$) stretch of $F_3^-$ in the $CsF_3$ ion pair. A Raman band at 389 $cm^{-1}$ was assigned to a higher salt complex. From the first observation of matrix-isolated $MF_3$ ion pairs, it took over 20 years until the free trifluoride ion ($F_3^-$) was first reported in mass-spectrometric studies[56,57] and another 10 years to the first observation of free $F_3^-$ in an IR spectroscopic study after co-deposition of laser-ablated transition metals with fluorine in solid argon and neon matrices.[58] IR bands at 511 $cm^{-1}$ in solid argon and at 525 $cm^{-1}$ in solid neon were assigned to the $\nu_3$ stretch of free $F_3^-$ whereby the observed band in neon was perfectly matched by the calculated anharmonic frequency at the CCSD(T)/aug-cc-pVTZ level of theory.[58] A natural population analysis (NPA) reported in that paper revealed that the negative charge of the $F_3^-$ ion is distributed over the terminal fluorine atoms. The

free trifluoride ion and its alkali ion pairs have been studied in a large number of further quantum-chemical investigations.[56–71] The reported experimental energy value for the dissociation of free $F_3^-$ [$(98 \pm 11)\,kJ\,mol^{-1}$][57] is in excellent agreement with the computed value at coupled cluster level ($110\,kJ\,mol^{-1}$)[62].

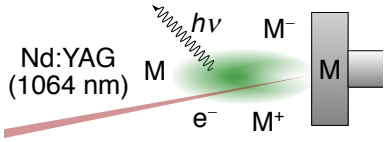


**Figure 1.5:** Illustration of the emissions produced during laser ablation of a metal target (M).

Figure 1.5 and Reactions (1.1) to (1.4) describe the proposed mechanisms that lead to the formation of free $F_3^-$ ions during co-deposition of laser-ablated metals with low concentrations of $F_2$ in an excess of noble gas.[7,59] Laser ablation first ionizes metal atoms of the metal target and produces metal cations and free electrons (1.1). At the same time UV radiation is emitted from the plasma plume which leads to homolytic cleavage of $F_2$ (1.2) and formation of $F^-$ atoms via an electron capture process (1.3). Free trifluorine anions ($F_3^-$) are then formed by the reaction of $F^-$ ions with $F_2$ molecules (1.4) during co-deposition in the rare gas matrix. It is important to note that $h\nu$ in Reaction (1.1) refers to the focused laser radiation, while in Reaction (1.2) it refers to UV radiation emitted by the plasma plume.

$$M \xrightarrow{h\nu} M^+ + e^- \tag{1.1}$$

$$F_2 \xrightarrow{h\nu} F + F \tag{1.2}$$

$$F + e^- \longrightarrow F^- \tag{1.3}$$

$$F^- + F_2 \longrightarrow F_3^- \tag{1.4}$$

In 2015 (Redeker, Beckers, Riedel; see Section 4.1) the matrix isolation of free $F_3^-$ and its alkali ion pairs was achieved by laser ablation of alkali fluorides.[72] In that study, the combination bands ($\nu_3 + \nu_1$) of free $F_3^-$ and $CsF_3$ in solid argon and krypton matrices were reported for the first time. With those combination bands it was possible to estimate the symmetric stretches ($\nu_1$) of $F_3^-$ and $CsF_3$ to appear above $381\,cm^{-1}$ and $373\,cm^{-1}$ in solid krypton and argon, respectively. This finding contradicted Ault's and Andrew's previous assignment of the $461\,cm^{-1}$ to the $\nu_1$ of $Cs^+F_3^-$. Since Ault and Andrews had observed bands at $461\,cm^{-1}$ and at $389\,cm^{-1}$ in their Raman spectra obtained after co-deposition of thermally vaporized CsF with $F_2$ in excess argon,[55] the $\nu_1$ band of $CsF_3$ was reassigned to the $389\,cm^{-1}$ in the 2015 report due to a better agreement with the experimental combination band and with the calculated CCSD(T)/def2-TZVPP value of $388\,cm^{-1}$.[59] In 2018, however, a quantum-chemical study by Henry F. Schaefer III and co-workers showed that although CCSD(T)/AWCVTZ calculations support the assignment of the $389\,cm^{-1}$ band, MRCISD+Q(4e,3o)/AVTZ calculations support the assignment of the $461\,cm^{-1}$ band to the $\nu_1$ stretch of $F_3^-$ in $CsF_3$.[70] Shortly after, Lester Andrews and Xuefeng Wang published

another study where they summarized all experimental and theoretical data on trifluorides. Supported by the multi reference configuration interaction (MRCI) results they assigned the 461 $cm^{-1}$ Raman band again to the symmetric $F_3^-$ stretch of $CsF_3$ and the band at 389 $cm^{-1}$ to the $\nu_1$ of free $F_3^-$, which they claim could be formed in several steps initiated by blue continuous wave laser two-photon ionization of caesium or rubidium atoms during Raman excitation using a blue argon ion laser.[73] If $F_2$ captures an electron produced by two-photon ionization of Cs and Rb this produces a free $F^-$ ion and a free F atom so that the free $F^-$ ion can react with further $F_2$ to yield $F_3^-$, according to Andrews and Wang.

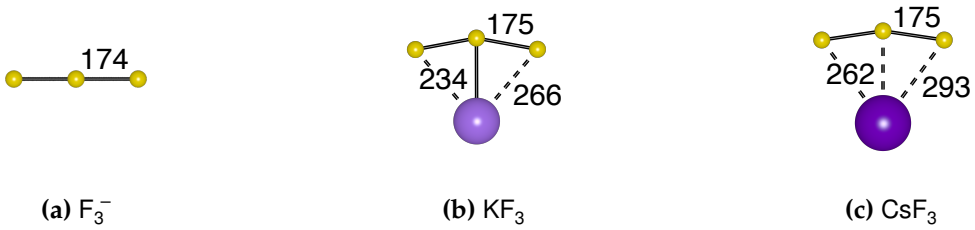


**(a)** $F_3^-$ **(b)** $KF_3$ **(c)** $CsF_3$

**Figure 1.6:** Molecular structures of $F_3^-$ and two selected $MF_3$ ion pairs calculated at the CCSD(T)/def2-TZVPP level of theory. Bond distances in pm.

Figure 1.6 shows the calculated CCSD(T)/def2-TZVPP structures of free and ion paired $F_3^-$. The free $F_3^-$ has $D_{\infty h}$ symmetry and almost retains its symmetry when interacting with an alkali cation, forming a T-shaped ion pair with $C_{2v}$ symmetry. The ion paired $F_3^-$ ion is only slightly bent (159°-163°) which explains why both, the free and the ion paired $F_3^-$ have only one stretching band ($\nu_3$) in the IR: in free $F_3^-$ the $\nu_1$ stretch is not IR active due to the rule of mutual exclusion and the bending of $F_3^-$ in $MF_3$ is small, so that its $\nu_1$ stretching band is not observed in the IR, either.

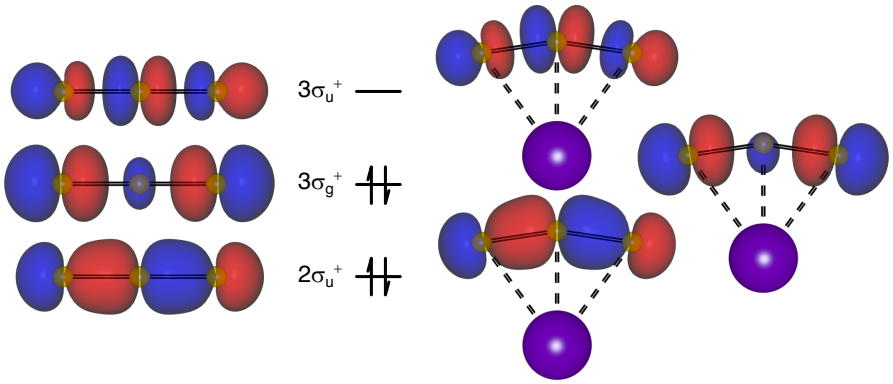


**Figure 1.7:** Sigma orbitals of $F_3^-$ involved in the 3-center 4-electron (3c-4e) bond at an isosurface of 0.05 $Å^{-3}$ of the free anion and its $Cs^+$ ion pair.

The bonding situation in the hypervalent trifluorine anion and other unperturbed $X_3^-$ ions (X = F, Cl, Br, I) is best described with a 3c-4e bond model as introduced by Pimentel and Rundle in 1951.[74,75] It can be seen as an extreme case of a dative bond[76,77] and yields three linear combinations of the $p_z$ orbitals of the three fluorine fragments as shown in Figure 1.7:

the lowest of these orbitals, a $\sigma_u^+$ orbital is the bonding orbital. The intermediate $\sigma_g^+$ orbital is the highest occupied molecular orbital (HOMO) of $X_3^-$ and is a non bonding orbital (for the $\pi$ orbitals see Figure 1.8). The third and highest $\sigma_u^+$ has strongly antibonding character and is the lowest unoccupied molecular orbital (LUMO) of $X_3^-$. The fact that the antisymmetric stretch of $MF_3$ (561 $cm^{-1}$) is observed 36 $cm^{-1}$ higher than that of free $F_3^-$ (525 $cm^{-1}$) in solid neon can be interpreted as evidence that the $F_3^-$ bond is strengthened by interaction with the cation, likely through delocalization of electrons from the HOMO. The full set of valence orbitals of $F_3^-$ can be found in Figure 1.8.

In contrast to the heavier halogens (Cl, Br, and I) not many higher polyfluorine anions are known. $F_5^-$ has supposedly been observed at 95 m/z in a gas-phase study[57] and in matrix-isolation IR investigations where bands at 851 $cm^{-1}$ and 1805 $cm^{-1}$ were assigned to the antisymmetric stretch and a combination band of V-shaped $F_5^-$ ($C_{2v}$), respectively.[7,59] However, the computed CCSD(T)/aug-cc-pVTZ ground state of $F_5^-$ has a hockey stick ($C_s$) structure, resembling an $F_2$ moiety coordinating to one end of an $F_3^-$ ion. Resolving this contradiction is the subject of ongoing experimental and theoretical efforts.

### The Trichlorine Anion

In 1967 G. C. Pimentel reported the detection of the $\nu_3$ band of the $^{35}Cl_3$ radical at 375 $cm^{-1}$ in a solid krypton matrix after passing a $Kr/Cl_2$ mixture through a microwave discharge.[78] Later, when the possibility of producing charged species by the microwave discharge method became increasingly clear, doubt was cast on Pimentels assignment. The possibility that the 375 $cm^{-1}$ band could be due to the free $Cl_3^-$ anion, was claimed, supported by the detection of a $Na^+Cl_3^-$ band at 375 $cm^{-1}$ in solid argon and under the assumption that $Na^+Cl_3^-$ can be described as a T-shaped ion pair consisting of an $Na^+$ cation and an asymmetric $Cl_3^-$ anion with $C_{\infty v}$ symmetry.[79–81] The alkali ion pairs of the trichloride ion ($Cl_3^-$) have been produced by co-deposition of thermally vaporized alkali chlorides (MCl) with chlorine in excess argon under cryogenic conditions[79,80] and the free ion as well as its alkali ion pairs have been the subject of quantum-chemical investigations.[82,83]

A number of crystal structures containing the trichlorine monoanion ($Cl_3^-$) are known today. In a crystalline environment with bulky counter cations like $[n\text{-}Pr_4N]^+$, $[(C_6H_5)_4As]^+$, $[(Me_2N)_2C_2N_4S_2Cl]^+$, $[(Me_2NC(Cl)N)_2SCl]^+$, $[(C_6H_5)_4P]^+$, $[n\text{-}Bu_4N]^+$, and $[Et_4N]^+$, $Cl_3^-$ adopts an almost linear structure, close to $D_{\infty h}$ symmetry, with bond angles between 177°-178° and almost equal Cl−Cl bonds ranging from 218-226 pm for the shorter and 231-239 pm for the longer bond.[84–90] The IR and Raman bands of $Cl_3^-$ of the known crystals are between 238-280 $cm^{-1}$. In the $[n\text{-}Pr_4N]^+$ crystal the trichloride ion has perfect $D_{\infty h}$ symmetry with a Raman band at 271 $cm^{-1}$, whereas in $[(C_2H_4Cl)(CH_3)_3N]^+Cl_3^-$ the $Cl_3^-$ ion has the lowest symmetry compared to all known $Cl_3^-$ crystal structures.[91] Another very asymmetric $Cl_3^-$ anion exists in the crystal structure of tetramethyl ammonium trichloride with Raman bands at 341 $cm^{-1}$ and 315 $cm^{-1}$.[1] Initially $[Me_4N]^+Cl_3^-$ was erroneously attributed to a $Cl_5^-$ salt due to a good

agreement of the experimental Raman bands with the calculated spectrum of the V-shaped pentachlorine anion ($Cl_5^-$).[90]

### Heteronuclear Trihalogen Anions

The first crystal structures of cesium dichlorido[92] and dibromido[93] iodate were reported by Ralph W. G. Wyckoff in 1920 and Linus Pauling in 1925, respectively. The crystal structure of ammonium chlorido bromido iodate $[H_4N]^+ClIBr^-$ has been reported by Rose C. L. Mooney in 1938.[94] Thereafter, many further X-ray diffraction (XRD), Raman and IR studies have been published on mixed trihalogen anions of I, Br, and Cl.[95–101] In the 1960s Karl O. Christe published Raman bands, IR bands, and powder X-ray diffraction (PXRD) patterns of the difluorido chlorate ion ($FClF^-$) with $Cs^+$, $Rb^+$, $K^+$, and $NO^+$ counter cations.[102–104] The first preparation of a cesium salt of $FBrF^-$ was reported in 1973.[105] Difluorido iodates ($FIF^-$)[106–108] and difluorido bromate ($FBrF^-$)[109] have both been prepared with larger organic counter cations in the late 1990s, but single crystal structures have, so far, only been obtained for $FIF^-$. Free heteroatomic trihalides $X_2Y^-$ (X, Y = Cl, Br, or I)[110] and $FXF^-$ (X = Cl, Br, and I)[108,111] have been quantum-chemically studied. A systematic theoretical investigation of free heteroatomic trihalogen anions (X = F-I) and their alkali ion pairs (M = Li-Cs and X = F-Br) is part of this thesis, see Section 4.3.

Molecular alkali ion pairs of chlorido bromates ($ClBrCl^-$, $BrClCl^-$, $BrClCl^-$)[80] and fluorido chlorates ($FClF^-$, $FClCl^-$)[9,55] as well as difluorido bromate ($FBrF^-$) and iodate ($FIF^-$)[112] have been isolated in argon matrices by Lester S. Andrews and co-workers. In all those studies, Knudsen cells were used for the vaporization of MX (X = Cl, Br, and I). The reactive gases were $Cl_2$, BrCl, and $Br_2$ in case of the chlorido bromates and $F_2$, ClF, and $Cl_2$ in case of the fluorido chlorates. Due to the lack of stability of BrF and IF, MFBrF and MFIF had to be produced by the reaction of $F_2$ with thermally vaporized MBr and MI, respectively. In those matrix-isolation studies some IR bands were also assigned to MXFF (X = Cl, Br, I)[112] and tentatively to MClFCl[55]. So far, free mixed trihalogen ions have not been successfully matrix-isolated. Andrews and co-workers who co-deposited laser ablated uranium with ClF in solid argon matrices tentatively assigned a band at 554 $cm^{-1}$ to the $\nu_3$ stretch of free $FClF^-$.[113] However, this assignment is not supported by state of the art quantum-chemical calculations (CCSD(T)/triple-$\zeta$) which predict the $\nu_3$ of $FClF^-$ to appear at 459 $cm^{-1}$.[111]

## 1.5 Second Row Homo-Triatomic Anions

The first row homo-triatomic anions from carbon to fluorine are all experimentally known, but vary extremely in stability, which makes them interesting to compare. Going from one to the next element in the row adds three more electrons to the molecular orbitals which leads to the situation that the first molecule in the row, $C_3^-$, with 13 valence electrons is a hypovalent open-shell molecule with a high bond order, whereas the last one, $F_3^-$, with 22

electrons is a hypervalent closed-shell molecule with a low bond order. Both $C_3^-$ and $F_3^-$ are very reactive and have only been characterized under cryogenic conditions. The azide anion ($N_3^-$) with 16 valence electrons has a closed shell and is the most stable of the four, since all N atoms have a complete octet of electrons. Azide anions are stable enough to be handled in water solution. Their sodium salts decompose at about 300 °C. The second most stable of the four is the ozonide anion, which is a 19 valence electron anion radical with a bent structure in accordance with the rules by Arthur D. Walsh for a 19 electron triatomic molecule.[114] $O_3^-$ can be handled in liquid ammonia at −40 °C[115] and its alkali salts are stable up to 55 °C ($CsO_3$), and tetramethyl ammonium ozonide ($[Me_4N]^+O_3^-$) even up to 75 °C.[116]

Figure 1.8 shows the valence orbitals of $C_3^-$, $N_3^-$, $O_3^-$ and $F_3^-$. By comparing the relative energies of their molecular orbitals it becomes immediately clear that the increase of nuclear charge and electronegativity in the direction from carbon to fluorine leads to a general lowering of the molecular orbitals in that direction. At the same time s- and p-orbitals get energetically and spatially more separated, decreasing the tendency of s- and p-orbitals to mix with each other.[117] E. g. the $1\sigma_u^+$ and $2\sigma_g^+$ orbitals of $C_3^-$ and $N_3^-$ and the $1b_1$ orbital of $O_3^-$ show significant sp-mixing, while the $2a_1$ orbital of $O_3^-$ and the $1\sigma_u^+$ and $2\sigma_g^+$ orbitals of $F_3^-$ show clear s-character. In the case of the tricarbon anion one unpaired electron is delocalized over the two degenerate non-bonding $1\pi_g$ orbitals which constitute the singly occupied molecular orbital (SOMO) of $C_3^-$. In $N_3^-$ these $1\pi_g$ orbitals constitute the HOMO and are fully occupied. Both $C_3^-$ and $N_3^-$ have a bond order of 2, with 4 fully occupied bonding orbitals ($1\sigma_g^+$, $1\sigma_u^+$, and $1\pi_u$), where the bonding character of $2\sigma_u^+$ is almost canceled by the antibonding character of $2\sigma_g^+$. The ozonide anion is bent and does not have degenerate orbitals. It has 4 fully occupied bonding orbitals ($1a_1$, $1b_1$, $2b_1$, $1b_2$), 4 fully occupied non-bonding orbitals ($3a_1$, $4a_1$, $3b_1$ and $1a_2$), 1 fully occupied ($2a_1$), and 1 partially occupied anti-bonding ($2b_2$, SOMO) orbital leading to a bond order of 1.25. The $F_3^-$ anion is by far the most weakly bound molecule in the row, with just 2 fully occupied bonding orbitals ($1\sigma_g^+$ and $2\sigma_u^+$), 8 fully occupied non-bonding orbitals ($1\sigma_u^+$, $1\pi_u$, $1\pi_g$, $2\pi_u$, and $3\sigma_g^+$), 1 fully occupied anti-bonding orbital ($2\sigma_g^+$), and a resulting bond order of 0.5.

The $C_3^-$ ion was reported in 1990 among other $C_n$ and $CsC_{2n}^-$ ($n \leqslant 10$) ions in mass spectra obtained from $Cs^+$ ion sputtering on a graphite target.[118] In 1997 Jan Szczepanski *et al.* co-deposited laser-ablated carbon atoms from a graphite rod with electrons from an electron gun in excess argon at 12 K. They reported a large number of carbon cluster anions and tentatively assigned a band at 1721.8 $cm^{-1}$ to the antisymmetric stretch of a free tricarbon monoanion $C_3^-$ with $D_{\infty h}$ symmetry.[119] In a subsequent study they reported the $^{12/13}C$ isotopic pattern of $C_3^-$ obtained by matrix isolation from a mixed isotope graphite target.[120] Several quantum-chemical studies have been reported on $C_3^-$ and other anionic carbon clusters.[121–124] The alkali tricarbide ion pairs ($MC_3$, M = Li, Na, K) have been predicted (B3LYP) to be the most stable alkali carbon clusters $MC_n$ (n = 1-10), but have not been reported experimentally, so far.[125]

The first high-resolution detection of the rovibrational gas-phase spectrum of the $\nu_3$ band

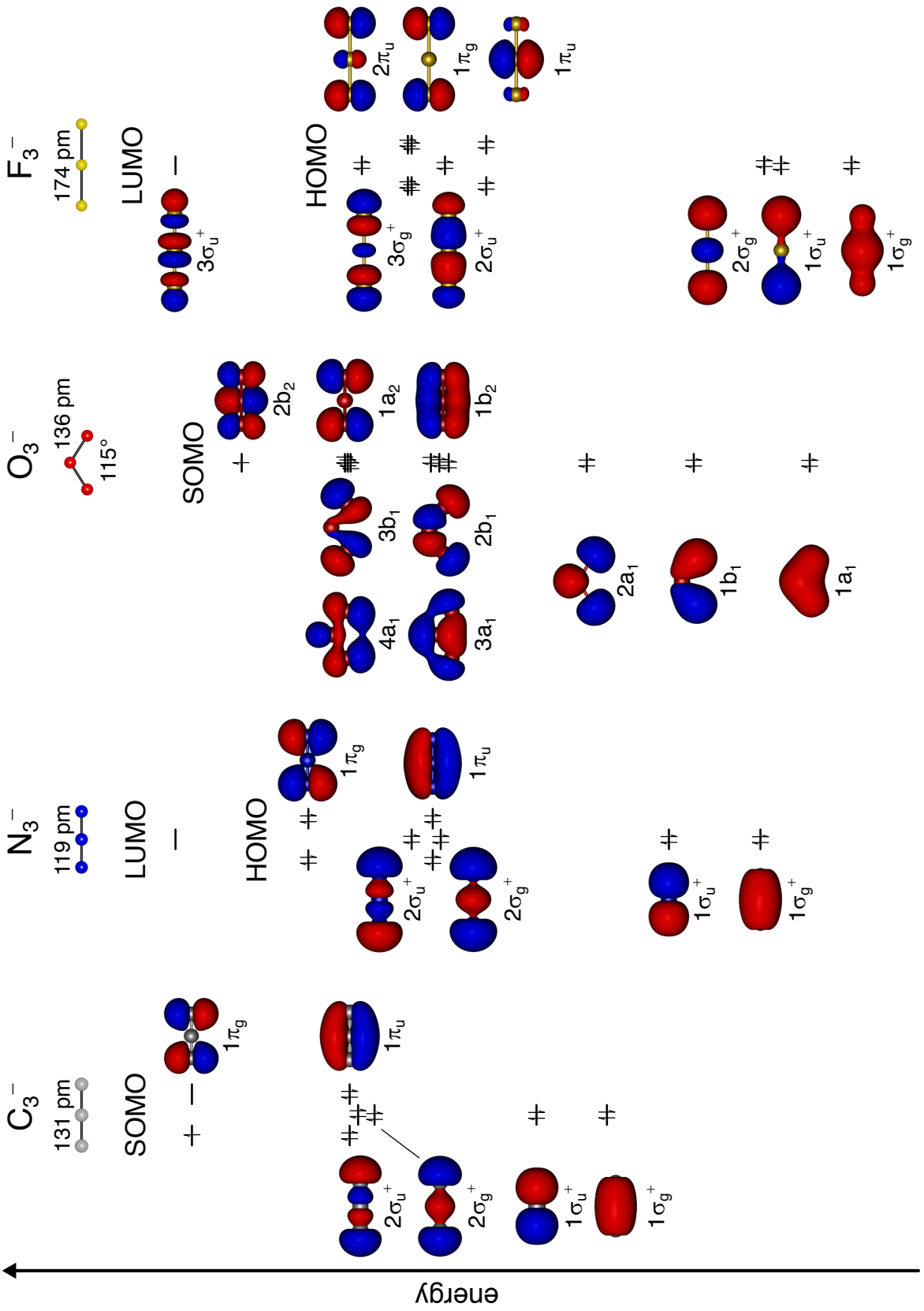


**Figure 1.8:** Calculated complete active space self consistent field (CASSCF) ($C_3^-$, $O_3^-$) and Hartree-Fock (HF) ($N_3^-$, $F_3^-$) molecular orbitals of second row homo-triatomic anions and their molecular structures calculated at the CCSD(T)/ma-def2-TZVP level of theory at an isosurface of 0.05 $Å^{-3}$.

of $N_3^-$ (1986.5 $cm^{-1}$) has been reported in 1987 where the azide ion was produced in an $NH_3/N_2O$ discharge.[126,127] A similar study of the corresponding $N_3$ radical was reported in the following year. It was obtained from the reaction of $HN_3$ with chlorine atoms from a discharge.[128] Electronic transitions and vibrational frequencies of alkaline earth azides were reported in a gas-phase study in 1988.[129] In the same year, matrix-isolated free trinitrogen radicals and monoanions were reported by Josef Michl and co-workers (1988) who bombarded a pure solid nitrogen ($N_2$) matrix with electrons and ions under cryogenic conditions.[130] They also postulated a metastable cyclic $N_3^-$ intermediate to explain the scrambling in their mixed isotope experiments.[131] Free linear $N_3$-radicals and anions have since been observed in a large number of matrix-isolation studies in which laser-ablated metals were co-deposited with pure nitrogen under cryogenic conditions.[132–148] Ion paired $N_3^-$ ions have been reported with Al, Ga, In, Tl, and Pt.[142,143,146] The rovibrational spectrum of the azide ion has been predicted with very high accuracy in a recent theoretical investigation.[149] Vibrational studies of alkali azides have been carried out for aqueous solutions[150] and for bulk material[151–153] such as powder and single crystals[154–156]. Due to the low decomposition temperatures of alkali azides below 400 °C,[157] matrix isolation by thermal vaporization or direct laser ablation of these salts is unlikely to work and a potentially dangerous endeavor.

The ozonide ion has been extensively studied in the gas phase[158–163] due to its role as an intermediate in the stratosphere and ionosphere[164]. Alkali ozonides are known by their crystal structures[115,165] and the electron density of $O_3^-$ in $KO_3$ has been determined experimentally.[166] Marilyn Jacox *et al.* were the first to measure IR spectra of molecular alkali ozonides isolated in solid argon matrices after co-deposition of $Ar/O_2/N_2O$ mixtures with thermally vaporized alkali metal atoms followed by photolysis.[167,168] Lester Andrews and co-workers studied the alkali ozonides ($MO_3$, M = Li-Cs) using IR and resonance Raman spectroscopy co-depositing thermally vaporized alkali metal atoms with ozone in an excess of argon at 15 K.[169–171] Later the free $O_3^-$ ion was observed after proton bombardment of oxygen ($O_2$) doped argon matrices[81,172], in gas-phase photodissociation spectra,[158,160] and after co-deposition of $O_3$/Ne mixtures with excited neon atoms from a microwave discharge.[173] The free ozonide ion[174–177] as well as the lithium,[176] sodium,[178] and potassium[179] ozonides have been the subject of high-level quantum-chemical studies.

## 1.6 Gold Fluorides and Fluorido Aurates

The first fluorine gold compound ever synthesized is gold trifluoride, $AuF_3$. It was produced by Henri Moissan in 1889, who heated elemental gold to 500-600 °C under a flow of fluorine gas.[180] In 1949 Alan G. Sharpe introduced a method to prepare gold trifluoride under mild conditions by the reaction of elemental gold with liquid $BrF_3$ leading to the formation of $AuF_3 \cdot BrF_3$ which can then be thermolysed above 120 °C to yield pure $AuF_3$ with only traces of bromine ($Br_2$) impurities.[181] It took almost another 20 years until the crystal structure of $AuF_3$ was solved. Crystalline $AuF_3$ consists of square planar $AuF_4$ units which are interconnected

via *cis*-coordinated Au−F···Au bridges to form a helical structure.[182,183] The structure of $AuF_3 \cdot BrF_3$ is similar to that of $AuF_3$ with alternating $AuF_4$ and $BrF_4$ units in the helix.[184] Other gold fluorides, $AuF_2$, $Au_2F_6$ and noble gas complexes of AuF have only been characterized in noble gas matrices under cryogenic conditions.[185,186] Free gold monofluoride has only been observed in mass spectrometric[187] and microwave spectroscopic[188] studies. The difluorido aurate ion ($AuF_2^-$) has been computed to be stable[189] and was observed in a mass spectrum as a decomposition product of $(CF_3)_2AuF_2$.[190] Tetrafluorido aurates ($AuF_4^-$) have been synthesized with a large number of mono- and dications.[191] Crystals of its alkali salts ($MAuF_4$, M = Li-Cs) have been characterized using XRD[192–195] and vibrational spectroscopy.[196,197] Similar to $AuF_4^-$, salts of the hexafluorido aurate ion ($AuF_6^-$) are known with a large variety of cations, including alkali cations[191,196] and represent the most stable form of gold in oxidation state +V. Monomolecular gold pentafluoride ($AuF_5$) has not been undoubtedly observed, yet, but has been reported as its dimer $Au_2F_{10}$.[198] Free $AuF_5$ is believed to be the strongest currently known Lewis acid[198] and has been computationally predicted to form an adduct even with difluorine ($F_2$)[199] to yield what had been reported as a gold heptafluoride, $AuF_7$, 20 years prior to its theoretical description[200].

# 2 Objectives

The aim of this work was the investigation of pulsed IR-laser deposition of non-volatile halides and pseudohalides, especially with respect to its suitability for the production and matrix isolation of free polyhalogen ions and their alkali ion pairs. Studying the formation, bonding and chemical properties of the isolated molecules experimentally and quantum-chemically was of special interest. The work can further be divided into three subgoals.

First, to study halogen bonding in trihalogen anions and their alkali ion pairs. Such adducts between halides and dihalogen molecules can be considered as the simplest examples for halogen bonding. Free trihalogen anions like $F_3^-$ and $Cl_3^-$ resemble the structure of trihalides extrapolated to infinitely weak interactions with a counter cation, whereas their corresponding alkali ion pairs reveal the structural properties of the trihalogen anions when paired with a strongly interacting cation.

Second, to get a deeper understanding of the processes that occur during the laser ablation of non-volatile salts by testing the suitability of the laser-ablation method for the matrix isolation of ternary salts. Laser-ablation products of potassium cyanide (KCN) were co-deposited with dihalogen/noble gas mixtures in order to see whether adducts between the pseudohalide $CN^-$ and dihalogens ($X_2$) are accessible via this technique.

Third, to further develop the method of salt laser ablation and to expand the spectrum of problems that can be addressed with this technique, mixtures of alkali fluorides (MF) with gold trifluoride ($AuF_3$) were studied using pulsed laser deposition and matrix isolation in order to investigate the formation of molecular alkali tetrafluorido aurates ($MAuF_4$) and the possibility of the formation of free fluorido aurate anions.

A Brief outline of the results obtained in this work is presented in the following chapter. For more information on the respective topics see the corresponding peer reviewed articles included in Chapter 4.

# 3 Outline

## 3.1 Trihalogen Anions and their Alkali Ion Pairs

The laser ablation of alkali halides (MX) provides unprecedented possibilities to study free anions next to their alkali ion pairs in matrix-isolation experiments as there is enough energy to enable separation of $M^+$ and $X^-$. However, MX is also homolytically cleaved during laser ablation and high amounts of the halogen radicals are formed. This leads to the formation of metal free anions, radicals and ion paired species during the co-deposition of laser-ablated salts with reactive gases in noble gas matrices.

### The Trifluorine Anion

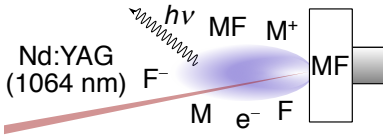


**Figure 3.1:** Illustration of the emissions produced during laser ablation of a metal fluoride target (MF).

$$MF \xrightarrow{h\nu} M^+ + F^- \tag{3.1}$$

$$MF \xrightarrow{h\nu} M + F \tag{3.2}$$

$$MF \xrightarrow{h\nu} MF_{(g)} \tag{3.3}$$

$$F^- + F_2 \longrightarrow F_3^- \tag{3.4}$$

$$MF + F_2 \longrightarrow MF_3^- \tag{3.5}$$

Figure 3.1 and Reactions (3.1) to (3.5) depict the formation of thr trifluorine anion and the alkali trifluoride by the reaction of laser ablated alkali fluoride (MF) with difluorine ($F_2$) in an excess of noble gas. Comparing the process of the formation of trifluoride, $F_3^-$, by laser ablation of alkali fluorides (MF) to the process from metal ablation (Section 1.4), it is most apparent that $F^-$ ions are readily available in the salt ablation plasma after heterolytic cleavage of MF (3.1). During metal ablation, $F_2$ gas first needs to be homolytically cleaved (1.2) so that the resulting F atoms can capture an electron to yield $F^-$ (1.3). This means, providing that heterolytic cleavage of MF during laser ablation is efficient, salt ablation should be the better source of free anionic polyfluorine anions ($F_n^-$) compared to metal

ablation. During laser ablation, MF is not only heterolytically cleaved. Homolytic cleavage (3.2) and vaporization of material (3.3) also takes place. Formation of $F_3^-$ and $MF_3$ proceeds via the reaction of $F^-$ (3.4) and MF (3.5) with difluorine ($F_2$) during deposition in the rare gas matrix, respectively. The *hν* in Reactions (3.1) to (3.3) refers to the focused laser radiation and not to the radiation emitted by the plasma plume.

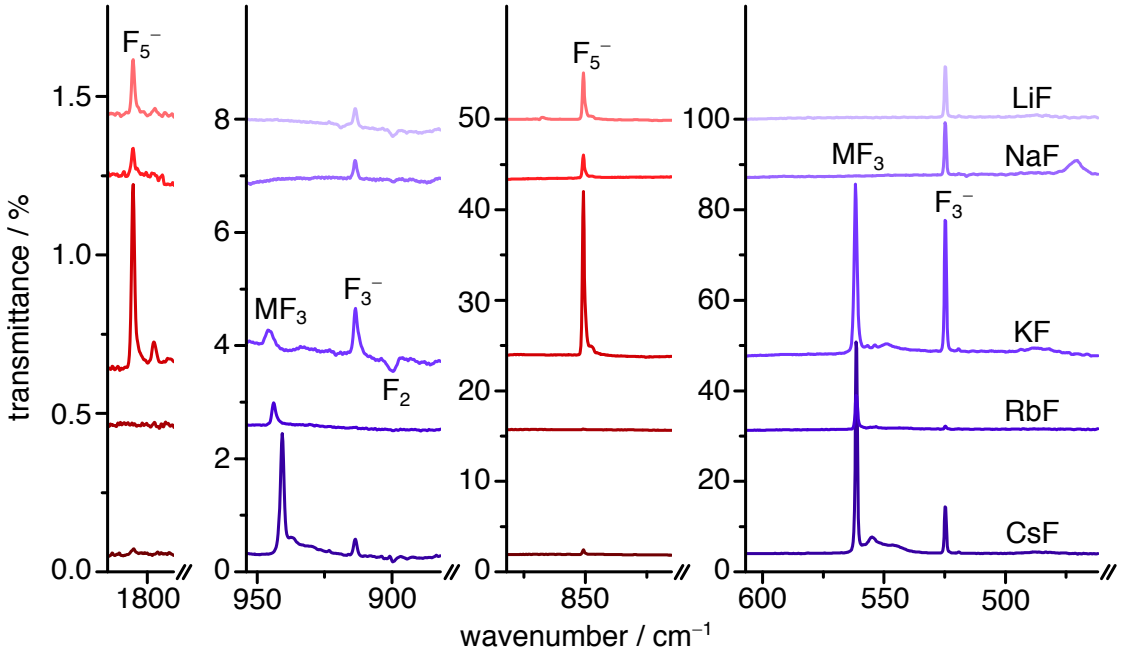


**Figure 3.2:** Difference IR spectra measured after co-deposition (1.25 h) of laser-ablated alkali fluorides MF (M = Li, Na, K, Rb, Cs) with 1 % $F_2$ in an excess of neon at 6 K and subsequent irradiation with light of $\lambda = 730$ nm (red) and $\lambda = 455$ nm (blue). Bands pointing upwards indicate depletion, bands pointing downwards formation of the corresponding species.

**Table 3.1:** IR band positions ($cm^{-1}$) of alkali trifluorides ($MF_3$) and the free trifluorine monoanion ($F_3^-$) matrix-isolated in solid neon at 6 K.

| Species | $\nu_3$ | $\nu_3 + \nu_1$ | $\nu_1$[a] |
|---|---|---|---|
| $F_3^-$ | 525 | 914 | > 389 |
| $KF_3$ | 561 | 946 | > 385 |
| $RbF_3$ | 561 | 944 | > 383 |
| $CsF_3$ | 561 | 941 | > 380 |
| $F_5^-$ | 851 | 1805 | > 954 |

[a] Predicted from $(\nu_3 + \nu_1) - \nu_3$.

Figure 3.2 shows IR difference spectra obtained after laser ablation of MF (M = Li, Na, K, Rb, Cs) with $F_2$ (1 %) in an excess of neon at 6 K and subsequent irradiation with red ($\lambda = 730$ nm) and blue ($\lambda = 455$ nm) light. Bands pointing upwards are depleted during irradiation. The bands depleted after irradiation with blue light are associated to the $\nu_3$

and $\nu_3 + \nu_1$ modes of $CsF_3$, $RbF_3$, $KF_3$, and free $F_3^-$, respectively. Like $\nu_3$, the $\nu_3 + \nu_1$ band is only observed for the ion pairs $MF_3$ with M = K, Rb, and Cs. For experiments with LiF and NaF, only free $F_3^-$ is observed. In the sequence $K < Rb < Cs$ the combination bands ($\nu_3 + \nu_1$) shift to lower wavenumbers, while the $\nu_3$ stretches remain virtually unchanged. This means that the $\nu_1$ band must be the carrier of the metal shift which can be explained considering symmetry: in the $MF_3$ molecule the $\nu_1$ stretch of the $F_3^-$ unit and the M−F stretch both have $a_1$ symmetry and therefore mix, whereas the $\nu_3$ stretch of the $F_3^-$ unit has $b_2$ symmetry and can therefore not mix with the M−F stretch. The combination bands at 941 $cm^{-1}$, 944 $cm^{-1}$, and 946 $cm^{-1}$ of $CsF_3$, $RbF_3$, and $KF_3$, respectively, in solid neon suggest that the corresponding symmetric stretches are expected slightly above 380 $cm^{-1}$, 383 $cm^{-1}$, and 385 $cm^{-1}$, respectively. The combination band of free $F_3^-$ at 914 $cm^{-1}$ suggests that the $\nu_1$ of $F_3^-$ will appear above 389 $cm^{-1}$, if anharmonicity is taken into account. The weak band at 900 $cm^{-1}$ that grows during photolysis ($\lambda = 455$ nm) indicates the formation of a perturbed $F_2$ unit and is a clear experimental evidence against the suggestion raised by Andrews and Wang[73], who doubted our assignment and claimed that the stretch of a perturbed difluorine molecule could serve as an alternative explanation for the observed combination band. In fact, the band assigned to the combination vibration of free $F_3^-$ and the F2 stretching band are clearly separated and show opposite behavior upon photolysis ($\lambda = 455$ nm) in solid neon. Furthermore, the new results obtained in solid neon show that the combination bands of the alkali trifluorides of caesium, rubidium, and potassium further support our assignment and contradict the assignment by Ault, Andrews, and Wang of the 461 $cm^{-1}$ Raman band to the symmetric $F_3^-$-stretch in $CsF_3$.[55,73] The deposition time of the above experiments of 1.25 h is significantly shorter than those needed for Knudsen effusion (24 h)[55] while yielding better results at the same time as evidenced by the observation of the combination bands which had not been observed using thermal vaporization of alkali fluorides.

After irradiation with red light two bands at 851 $cm^{-1}$ and 1805 $cm^{-1}$ were depleted. These bands were previously observed after co-deposition of laser-ablated metals with low amounts of fluorine ($F_2$) in solid neon and were assigned to the $\nu_3$ stretch and the $\nu_3 + \nu_1$ combination band, respectively, of a V-shaped ($C_{2v}$) pentafluorine anion ($F_5^-$)[7,59]. However, this assignment is still subject to ongoing investigation as it disagrees with quantum-chemical calculations[58] which predict for $F_5^-$ a hockey-stick like ($C_s$) structure with a perturbed $F_2$ unit coordinating to an $F_3^-$ moiety. Using laser ablation of alkali fluorides (Figure 3.2) the same bands were reproduced in extraordinarily high yields. The fact that the 851 $cm^{-1}$ band is also observed in experiments with lithium and sodium fluoride, which do not form $MF_3$ ion pairs, supports the assignment of the 851 $cm^{-1}$ band to a free polyfluoride anion. Furthermore, it could be shown that the bands associated to the $F_3^-$ ion are completely depleted upon irradiation with ultraviolet (UV) light ($\lambda = 273$ nm) while the supposed $F_5^-$ bands are not affected by this radiation (not shown in Figure 3.2). Based on these results the assignment of the 851 $cm^{-1}$ band to a perturbed $F_2$-stretch of a hockey-stick shaped $F_5^-$ can be ruled out, since its predicted strong $F_3^-$-stretch at around 525 $cm^{-1}$ is missing.

Solving the contradiction between experimental and computational results for the $F_5^-$ ion is still subject of an ongoing investigation.

### The Trichlorine Anion

Co-deposition of laser-ablated alkali chlorides (MCl, M = Cs, Rb, K, Na) with dichlorine ($Cl_2$) in solid neon matrices at 6 K led to the observation of free $Cl_3^-$ ions and the corresponding ion pairs $MCl_3$ (Section 4.2). The antisymmetric stretch ($\nu_3$) of free $Cl_3^-$ was observed at 252 $cm^{-1}$ in neon as well as in argon and is in good agreement with the calculated value by Dixon *et al.* (254 $cm^{-1}$, CCSD(T)/aug-cc-pVTZ)[82]. The observation of the antisymmetric stretch of $Cl_3^-$ at 252 $cm^{-1}$ clearly supports Pimentel's previous assignment of the 375 $cm^{-1}$ IR band in solid krypton[78] to the symmetric stretch of the $Cl_3$ radical. Using high-level quantum-chemical calculations it could further be elucidated why the 375 $cm^{-1}$ band observed for the sodium trihalide ion pair in solid argon[79–81] is shifted to such high wavenumbers. Figure 3.3 shows the structures of free $Cl_3^-$, sodium trichloride ($NaCl_3$) and caesium trichloride ($CsCl_3$) calculated at the CCSD(T)/def2-TZVPP level of theory. Comparison of the structures shows that the interaction of the $Cl_3^-$ ion with a cation leads to a heavy distortion of the Cl−Cl bonds so that $NaCl_3$ is better described as an NaCl···$Cl_2$ adduct rather than an $Na^+Cl_3^-$ ion pair. The calculated bond length of the shorter Cl−Cl bond in $NaCl_3$ is closer to the calculated bond length of the dichlorine molecule ($Cl_2$, 201 pm, CCSD(T)/def2-TZVPP) than to the bond length of free $Cl_3^-$. This distortion leads to perturbed $Cl_2$ stretches of $NaCl_3$ at 389 $cm^{-1}$ and at 375 $cm^{-1}$ in solid neon and argon, respectively. Due to a limitation of the spectral range to >180 $cm^{-1}$ by the CsI window used for FIR measurements it was not possible to detect the stretching mode of the longer Cl···Cl bond of $NaCl_3$ which is expected to occur around 108 $cm^{-1}$ (CCSD(T)/def2-TZVPP). However, the $Cl_3^-$ anion in $MCl_3$ becomes increasingly symmetric going to larger alkali cations (M = K, Rb, Cs) so that the perturbed $Cl_2$ stretch shifts to lower wavenumbers. At the same time the longer Cl···Cl stretch shifts to higher wavenumbers and was therefore observed for $CsCl_3$ and $RbCl_3$ in solid neon and argon matrices (Table 3.2). Although the $Cl_3^-$ anion in $MCl_3$ gets more symmetric when paired with heavier alkali metals in $CsCl_3$ it is still more asymmetric than in most of the known trichloride crystal structures.[84–90]

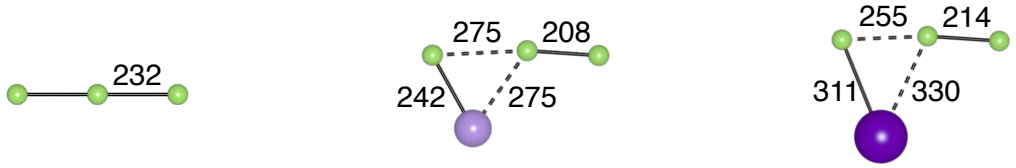


**(a)** $Cl_3^-$ **(b)** $NaCl_3$ **(c)** $CsCl_3$

**Figure 3.3:** Molecular structures of $Cl_3^-$ and two selected $MCl_3$ ion pairs calculated at the CCSD(T)/def2-TZVPP level of theory. Bond distances in pm.

**Table 3.2:** Vibrational band positions ($cm^{-1}$) of the $Cl_3^-$ anion and its alkali ion pairs.[a]

| Species | $\nu_3$ | $\nu_1$ | Medium | Reference |
|---|---|---|---|---|
| $Cl_3^-$ | 252 | *n. o.* | neon | this work |
| | 252 | *n. o.* | argon | this work |
| | 254 | 261 | calc.[b] | [82] |
| $CsCl_3$ | 339 | 218 | neon | this work |
| | 327 | 225 | argon | [79, 80] |
| | 347 | 215 | calc.[c] | this work |
| $RbCl_3$ | 343 | 223 | neon | this work |
| | 340 | 223 | argon | [79, 80] |
| | 347 | 223 | calc.[c] | this work |
| $KCl_3$ | 352 | *n. o.* | neon | this work |
| | 345 | *n. o.* | argon | [79, 80] |
| | 361 | 139 | calc.[c] | this work |
| $NaCl_3$ | 389 | *n. o.* | neon | this work |
| | 375 | *n. o.* | argon | [79, 80] |
| | 417 | 108 | calc.[c] | this work |

[a] In the case of the alkali ion pairs ($MCl_3$) $\nu_3$ and $\nu_1$ refer to the perturbed $Cl_2$ stretch and the longer Cl···Cl stretch, respectively; *n. o.* – not observed. [b] CCSD(T)/aug-cc-pVTZ. [c] CCSD(T)/def2-TZVPP.

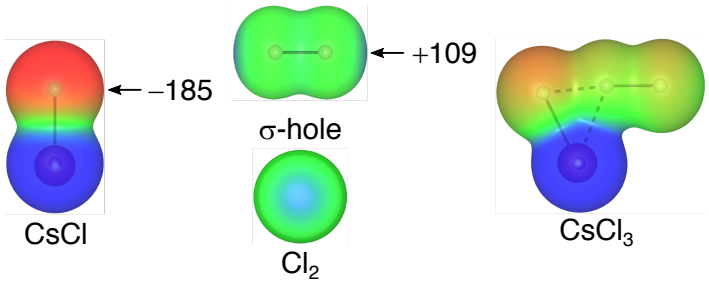


**Figure 3.4:** electrostatic potential (ESP) maps of CsCl, $Cl_2$, and $CsCl_3$ from −0.1 $E_h$ (red) to 0.1 $E_h$ (blue) on the electron isosurface of 0.003 electrons $bohr^{-3}$ calculated at the B3LYP/def2-TZVPP level of theory. The numbers indicate the electrostatic potential ($kJ\,mol^{-1}$) on the electron density isosurface of 0.001 electrons $bohr^{-3}$ at the positions shown.

In order to rationalize the reactivity of alkali halides with dihalogens it is helpful to look at the electrostatic potentials of those compounds. Figure 3.4 shows ESP maps of CsCl and $Cl_2$ before and after the formation of $CsCl_3$. The image clearly shows the highly negative potential (red) around the chloride ion of CsCl and the sigma hole (blue) of the dichlorine molecule ($Cl_2$). The term sigma hole describes the points of highest positive electrostatic potential at an extension on the bond axis of the $Cl_2$ molecule. After the formation of $CsCl_3$ the negative electrostatic potential initialy at $Cl^-$ becomes distributed over the whole $Cl_3^-$ moiety

where it is mainly located at the terminal chlorine atoms. From Figure 3.3b, 3.3c and 3.4 it further becomes apparent that there is also an interaction between the positively charged alkali metal cation and the slight negative electrostatic potential in the xy-plane around the intermediate chlorine atom causing the trichloride ion to slightly bend.

### Heteronuclear Trihalogen Anions

Alkali ion pairs of mixed trihalides of bromine, chlorine and fluorine were also investigated using high-level quantum-chemical calclulations (CCSD(T)/def2-TZVPP) in order to systematically understand the requirements of the formation of such trihalides and to see which combinations are stable and which are not (for details see Section 4.3).

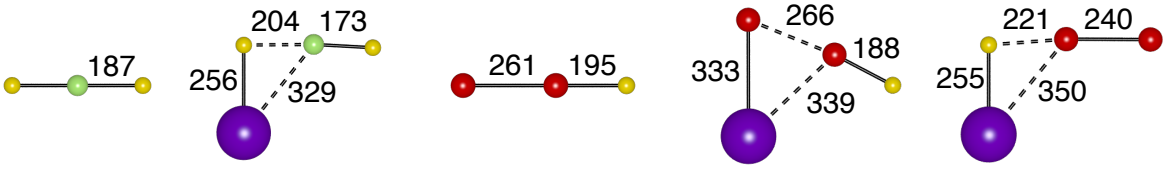


**(a)** $FClF^-$ **(b)** CsFClF **(c)** $BrBrF^-$ **(d)** CsBrBrF **(e)** CsFBrBr

**Figure 3.5:** Molecular structures of two selected mixed trihalogen anions and their corresponding caesium ion pairs calculated at the CCSD(T)/def2-TZVPP level of theory. Bond distances in pm.

In general it could be shown that the strength of a halogen bond in an alkali trihalide (MXYX) increases with the sigma hole of the dihalogen XY and with the strength of the negative electrostatic potential of the electron donating halide in MX (c. f. Figure 3.4). In the light of the new calculations the assignments of IR bands to MXFF (X = Cl, Br, I)[112] and MClFCl[55] species in previous matrix-isolation studies seem unlikely. For example, to form KBrFF from the reaction of KBr and $F_2$ it would be necessary to form a halogen bond between $Br^-$ and the sigma hole of fluorine (c. f. Figure 3.4). However, $Br^-$ is expected to be oxidized by $F_2$. The reaction of KCl with ClF to yield KClFCl is even less plausible since the fluorine atom in ClF has a negative electrostatic potential where dihalogens usually have a sigma hole. The reason for those assignments was the erroneous claim that alkali ion pairs of $FClF^-$, $FBrF^-$, and $FIF^-$ were T-shaped with a $C_{2v}$ symmetric structure. In such an ion pair only the $\nu_3$ stretch of $FXF^-$ could be observed in the IR whereas the $\nu_1$ stretch would be IR inactive. Therefore, the additional bands were assigned to the other trihalide species MXFF. However, quantum-chemical calculations at the CCSD(T) level of theory show that only the alkali trifluorides $MF_3$ have a $C_{2v}$ structure (1.6). All other alkali trihalides have $C_s$ symmetry (see Figure 3.5) and should therefore have two IR-active stretching bands, one stretch for the longer and one stretch for the shorter XF-bond. With those results, it was also possible to reassign the bands previously misassigned to the unlikely structures MXFF and MClFCl to the XF-stretch associated with the longer XF-bond in the corresponding MFXF ion pairs, as well

as to the ClCl-stretch in MClClF, respectively. The CCSD(T) calculations further showed that alkali trihalide structures of the types MFFX, MXFF, and MXFX do not converge in any case. Figure 3.5 shows the structures of two selected mixed trihalides and their corresponding caesium ion pairs.

## 3.2 Potassium Tricarbide and Potassium Azide

The cyanide anion ($CN^-$) is a pseudohalide and is expected to behave similarly to other halides in a way that it forms halogen bonds with dihalogen molecules ($X_2$) where $CNXX^-$ ions are produced. In order to find a viable route to produce such anions under cryogenic conditions, the products of laser-ablated KCN were isolated in solid neon and argon matrices to see whether free $CN^-$ ions for further reactions with dihalogens are formed. Surprisingly, no $CN^-$ ions were observed in such spectra. Instead, a large number of polycarbon and polynitrogen species could be isolated including the novel potassium ion pairs $KC_3$ and $KN_3$. Potassium tricarbide ($KC_3$) has a $C_{2v}$ minimum structure whereas molecular potassium azide ($KN_3$) was found to exist as an end-on ($C_{\infty v}$) and a side-on ($C_{2v}$) isomer (Figure 3.6). In addition, a comprehensive set of reaction mechanisms could be derived from the analysis of the IR spectra obtained after co-deposition of laser ablated potassium cyanide with excess noble gas, which explain the formation of most of the observed products. For details see Section 4.4 main text and Supporting Information (SI).

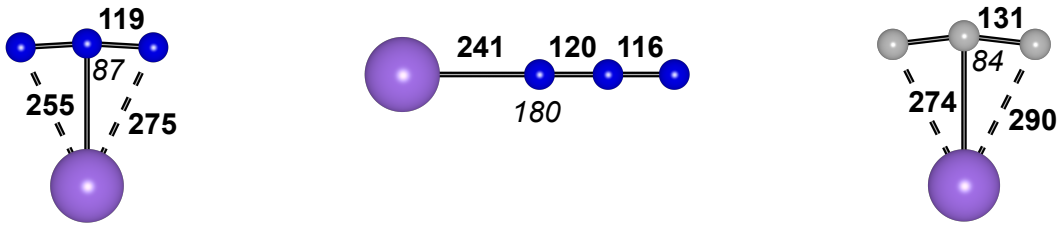


**(a)** $KN_3$ ($C_{2v}$) **(b)** $KN_3$ ($C_{\infty v}$) **(c)** $KC_3$ ($C_{2v}$)

**Figure 3.6:** Molecular structures of $KN_3$ and $KC_3$ calculated at the CCSD(T)/ma-def2-TZVP level of theory. **Bold** numbers indicate bond distances in pm. *Italic* numbers indicate bond angles in deg.

Figure 3.7 shows IR spectra obtained after co-deposition of different laser-ablated KCN isotopologues (a-c) and of laser ablated NaCN (d) with argon at 12 K. The spectra show the metal independent $\nu_3$ stretch of free $C_3^-$ which is known from the literature[119,120] and a new metal dependent band which could be assigned to the antisymmetric stretch ($\nu_3$) of the $C_3^-$ unit in the ion pair $KC_3$. For exact band positions see Table 3.3 and Section 4.4. Both free $C_3^-$ and the $KC_3$ ion pair reveal a sextet in mixed $^{12/13}C$ isotope experiments (see Section 4.4 SI) indicating that the ion pair has $C_{2v}$ symmetry. Calculations at the CCSD(T)/ma-def2-TZVP

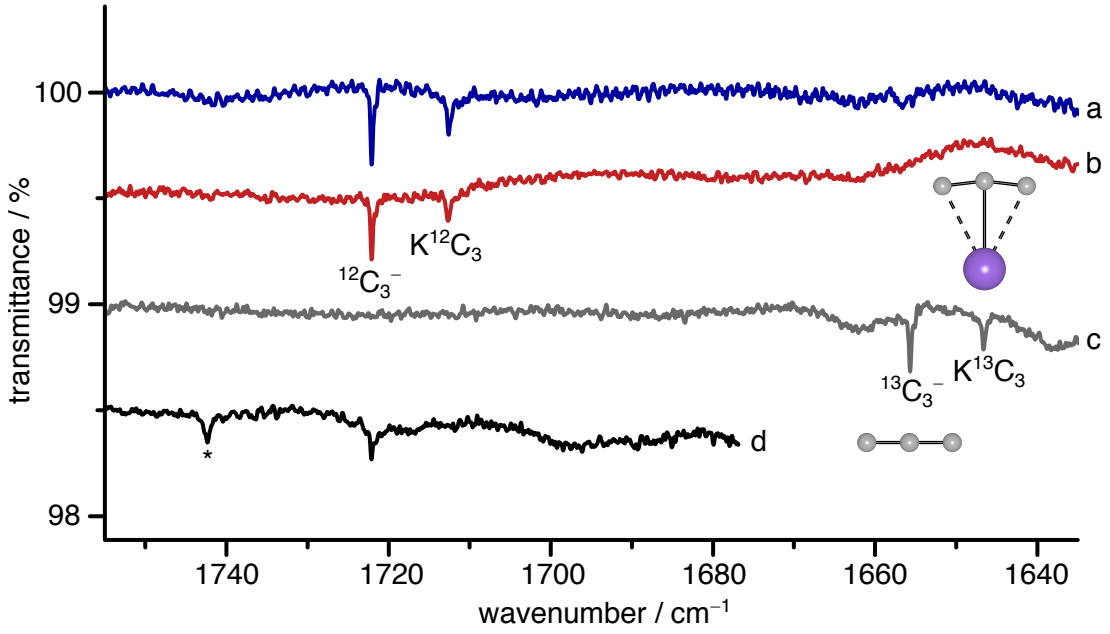


**Figure 3.7:** IR spectra in the $\nu_3$ region of $C_3^-$ obtained after co-deposition of a) KCN, b) $KC^{15}N$, c) $K^{13}CN$, and d) NaCN in excess argon at 12 K. * Unknown band.

level also show a side-on minimum structure ($C_{2v}$) whereas the end-on isomer is predicted to be a first order transition state. The ion pair $KC_3$ is expected to be formed during sample deposition by the reaction of KC and $C_2$ (3.9). Potassium monocarbide (KC) is formed during laser ablation of KCN by removal of a nitrogen atom (3.6) whereas $C_2$ is expected to be formed by recombination of two carbon atoms (3.8) obtained from reaction (3.7).

$$KCN \xrightarrow{h\nu} KC + N \tag{3.6}$$

$$KCN \xrightarrow{h\nu} KN + C \tag{3.7}$$

$$C + C \longrightarrow C_2 \tag{3.8}$$

$$KC + C_2 \longrightarrow KC_3 \tag{3.9}$$

Figure 3.8 shows difference IR spectra obtained from laser-ablated $KC^{14/15}N$ isotopologues with traces of $^{14/15}N_2$ in an excess of neon at 6 K. It shows two bands that are formed during irradiation with blue light ($\lambda = 470$ nm). For the exact IR band positions see Table 3.3 and Section 4.4. The difference spectrum after irradiation with UV light (Figure 3.8d) shows that the band around 2071 $cm^{-1}$ is converted into the band around 1998 $cm^{-1}$ upon irradiation with $\lambda = 273$ nm. This implies that these two bands belong to two different species. The different isotope patterns of the two species in the mixed isotope experiment (Figure 3.8c) further allowed for an assignment of the bands to an end-on ($C_{\infty v}$) and a side-on ($C_{2v}$) isomer of $KN_3$. End-on $KN_3$ reveals an octet in the mixed isotope experiment, whereas side-on $KN_3$ shows only a sextet, since the isotopologues $^{14}N^{14}N^{15}N$ and $^{15}N^{14}N^{14}N$, as well as $^{15}N^{15}N^{14}N$ and $^{14}N^{15}N^{15}N$, respectively, are chemically equivalent in the side-on isomer but not in the end-on isomer.

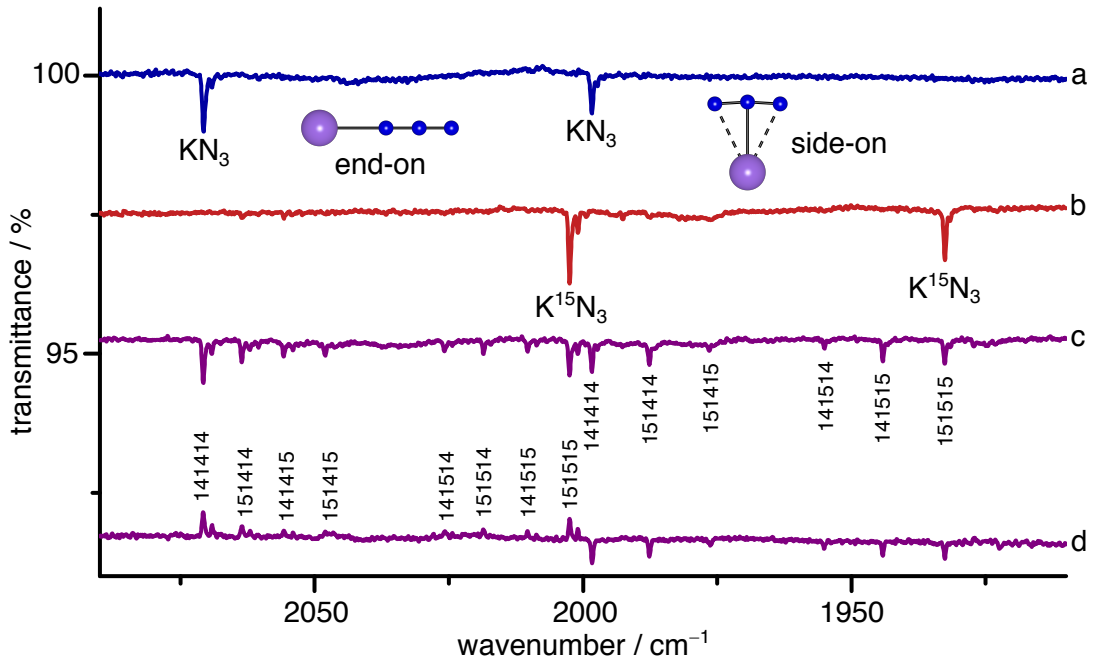


**Figure 3.8:** Difference IR spectra in the $\nu_3$ region of $N_3^-$ obtained after co-deposition in excess neon at 6 K and irradiation ($\lambda = 470$ nm) of a) KCN with traces of $N_2$, b) $KC^{15}N$ with traces of $^{15}N_2$, c) KCN/$KC^{15}N$ (1:1) with traces of $N_2/^{15}N_2$ (1:1), and d) after irradiation of c with $\lambda = 273$ nm. Bands pointing downwards indicate formation, bands pointing upwards depletion of the corresponding species.

Three reaction mechanisms were considered for the formation of molecular $KN_3$: i) the recombination of $K^+$ and $N_3^-$ ions, ii) the reaction of potassium atoms (K) with $N_3$ radicals, and iii) the reaction of potassium nitrene (KN) with dinitrogen ($N_2$) molecules (3.10). The former two reaction paths could be ruled out for argon and neon matrices since neither $N_3^-$ ions nor $N_3$ radicals could be observed in these deposits. Thus, the formation of $KN_3$ after irradiation implies that the potential interstellar species KN in its triplet ground state is present in the deposit and reacts with $N_2$ by photo excitation and intersystem crossing (ISC) to its lowest lying singlet state.

$$KN + N_2 \xrightarrow{h\nu} KN_3 \tag{3.10}$$

The isotope patterns of $KN_3$ obtained after photolysis ($\lambda = 470$ nm) of laser-ablated $KC^{14}N$ and $KC^{15}N$ with $^{15}N_2$ and $^{14}N_2$, respectively, co-deposited with solid neon led us to assume that the reaction proceeds via a cyclic $K(\eta^3\text{-}N_3)$ intermediate or transition state (3.11) similar to the transient cyclic $N_3^-$ postulated by Michl and co-workers.[131]

$$K^{14}N + {}^{15}N_2 \xrightarrow{h\nu} K(\eta^3\text{-}{}^{14}N^{15}N_2) \longrightarrow K^{14}N^{15}N^{15}N \text{ or } K^{15}N^{15}N^{14}N \text{ or } K^{15}N^{14}N^{15}N \tag{3.11}$$

Quantum-chemical calculations at the CCSD(T)/ma-def2-TZVP level of theory predict that the side-on isomer of $KN_3$ is thermodynamically favored over the end-on isomer by about 3.5 kJ mol$^{-1}$. The computed barrier for the rearrangement of the end-on to the side-on

**Table 3.3:** Calculated and experimental vibrational band positions ($cm^{-1}$) of second row triatomic anions and their potassium ion pairs.[a]

| Species | $\nu_3$ | $\nu_2$ | $\nu_1$ | Medium | Reference |
|---|---|---|---|---|---|
| $C_3^-$ ($^2\Pi_g$) | 1722 | *n. o.* | *n. o.* | argon | [119, 120]; this work |
| | 1769 | 371, 205 | *n. a.* | calc.[b] | [124] |
| | 1741 | 402, 263 | 1172 | calc.[c] | this work |
| $KC_3$ ($C_{2v}$) | 1713 | *n. o.* | *n. o.* | argon | this work |
| | 1727 | 440, 186 | 1182 | calc.[c] | this work |
| $N_3^-$ ($^1\Sigma_g^+$) | 1986 | *n. o.* | *n. o.* | gas | [126, 127] |
| | 1992 | *n. o.* | *n. o.* | argon | [142] |
| | 2004 | *n. o.* | *n. o.* | $N_2$ | [130, 131]; this work |
| | 2042 | 640 | 1310 | calc.[d] | [149] |
| $KN_3$ ($C_{\infty v}$) | 2071 | *n. o.* | 1345 | neon | this work |
| | 2057 | *n. o.* | *n. o.* | argon | this work |
| | 2049 | *n. o.* | *n. o.* | $N_2$ | this work |
| | 2124 | 643, 550 | 1358 | calc.[c] | this work |
| $KN_3$ ($C_{2v}$) | 1998 | *n. o.* | *n. o.* | neon | this work |
| | 1989 | *n. o.* | *n. o.* | argon | this work |
| | 2007 | *n. o.* | *n. o.* | $N_2$ | this work |
| | 2039 | 678, 630 | 1301 | calc.[c] | this work |
| $O_3^-$ ($^2B_2$) | 797 | 550 | 975 | gas | [158–160, 162, 163] |
| | 796 | *n. o.* | *n. o.* | neon | [173] |
| | 804 | *n. o.* | *n. o.* | argon | [81, 172] |
| $KO_3$ ($C_{2v}$) | 786 | 601 | 1004 | argon | [169–171] |
| | 895 | 619 | 1062 | calc.[e] | [179] |
| $F_3^-$ ($^1\Sigma_g^+$) | 525 | *n. o.* | > 389[f] | neon | [58, 59]; this work |
| | 511 | *n. o.* | 389 | argon | [55, 58, 73] |
| | 517 | *n. o.* | *n. a.* | $N_2$ | [72] |
| | 512 | *n. o.* | > 377[f] | krypton | [72] |
| | 523 | 254 | 397 | calc.[g] | [58] |
| $KF_3$ ($C_{2v}$) | 561 | *n. o.* | > 385[f] | neon | [59]; this work |
| | 551 | *n. o.* | 461, 389 | argon | [55] |
| | 586 | 225, 200 | 408 | calc.[h] | [59] |
| | 602 | 231, 210 | 488 | calc.[i] | [70] |

[a] *n. o.* – not observed; *n. a.* – not available. [b] B3LYP/aug-cc-pVTZ (harm.). [c] CCSD(T)/ma-def2-TZVP (harm.). [d] CCSD(T)/aug-cc-pV6Z (harm.). [e] CCSD(T)/6-311G(2df)(K);6-311+G(2df)(O) (harm.). [f] Predicted from $(\nu_3 + \nu_1) - \nu_3$. [g] CCSD(T)/aug-cc-pVQZ (anharm.). [h] CCSD(T)/def2-QZVPP (harm.). [i] MRCISD+Q(4e,3o)/aug-cc-pVTZ (harm.).

isomer is 12.5 kJ mol$^{-1}$ and appears to be high enough to not be surmounted by annealing of the deposit.

Due to the new results for $KC_3$ and $KN_3$ the effects that the interaction with alkali cations has on the triatomic anions can now be compared within the group of second row triatomic anions. Table 3.3 summarizes the most accurate experimental and calculated data available on homoatomic second row triatomic anions from carbon to fluorine and their potassium ion pairs. The interaction of $C_3^-$ with $K^+$ leads to a red shift of $\nu_3$ of 10 cm$^{-1}$ while the calculated (CCSD(T)/ma-def2-TZVP) bond length of 131 pm remains the same. The interaction of $K^+$ with $N_3^-$ has no significant effect in the case of side-on $KN_3$ which is in agreement with an unchanged bond length (CCSD(T)/ma-def2-TZVP) of 119 pm in both the free azide and the side-on ion pair. For the end-on isomer of $KN_3$ the antisymmetric stretch is strongly blue shifted while the calculated average N−N bond length only decreases from 119 pm to 118 pm. The $\nu_3$ stretch of $O_3^-$ shifts about 20 cm$^{-1}$ to lower wavenumbers upon interaction with $K^+$ while the $\nu_1$ stretch exhibits a blue shift of about 30 cm$^{-1}$. The trifluoride $\nu_3$ stretch of $KF_3$ is strongly blue shifted by about 40 cm$^{-1}$ compared to the free anion. Reasons for such shifts can be the weakening or strengthening of bonds by changes in the population of bonding and antibonding orbitals caused by the cation, changes to the bond angle can lead to a different coupling between $\nu_3$ and $\nu_1$, and even vibronic coupling may play a role.

## 3.3 Alkali Tetrafluorido Aurates

By laser ablation of mixed salt targets with low amounts of $AuF_3$ (2-3 %) in excess alkali fluoride (MF) it was possible to isolate the molecular alkali tetrafluorido aurates in neon matrices at 6 K. For details see Section 4.5 main text and SI.

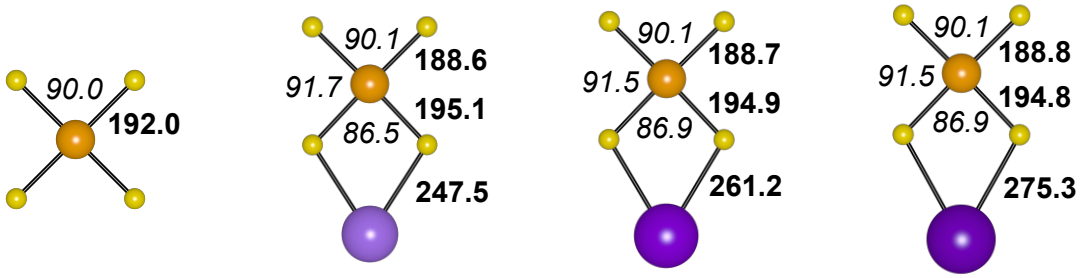


**(a)** $AuF_4^-$ ($D_{4h}$) **(b)** $KAuF_4$ ($C_{2v}$) **(c)** $RbAuF_4$ ($C_{2v}$) **(d)** $CsAuF_4$ ($C_{2v}$)

**Figure 3.9:** Molecular structures of $AuF_4^-$ calculated at the CCSD(T)/def2-TZVPPD level of theory and of $MAuF_4$ with M = K, Rb and Cs calculated at the CCSD(T)/def2-TZVPP level of theory. **Bold** numbers indicate bond distances [pm]. *Italic* numbers indicate bond angles [°].

The IR bands obtained from these deposits excellently matched the trends in the Au−F bonds predicted for the tetrafluorido ion pairs of potassium, rubidium, and caesium calculated at the CCSD(T)/def2-TZVPP level of theory (Figure 3.9). The free $AuF_4^-$ has $D_{4h}$

symmetry with four equally long Au−F bonds. When $AuF_4^-$ interacts with an alkali cation, its symmetry is decreased to $C_{2v}$ symmetry with two shorter terminal Au−F bonds and two longer bridging Au−F bonds compared to the free $AuF_4^-$ ion. The terminal Au−F bonds are further predicted to be slightly elongated in the sequence K < Rb < Cs while the bridging Au−F get slightly shorter, matching the trend of decreasing Lewis acidity of the corresponding cations in that direction. In the experimental spectra the two vibrational bands for the terminal F−Au−F moiety are red shifted and the two observed bands for the bridging F−Au−F moiety are blue shifted for the heavier alkali metals Cs and Rb compared to K. In addition, by the co-deposition of laser-ablated $MF/AuF_3$ mixtures in an excess of neon, bands of the $AuF_3$ monomer and its dimer $Au_2F_6$ were obtained. These bands have already been reported previously after co-deposition of laser-ablated gold with $F_2$ in neon and argon.[185] However, the spectra obtained in this work by laser ablation of an $MF/AuF_3$ mixture show much stronger and nicely resolved bands which allowed for the first assignment of the complete set of $Au_2F_6$ stretching frequencies.

# 4 Publications

## 4.1 Investigation of Alkali Metal Polyfluorides by Matrix-Isolation Spectroscopy

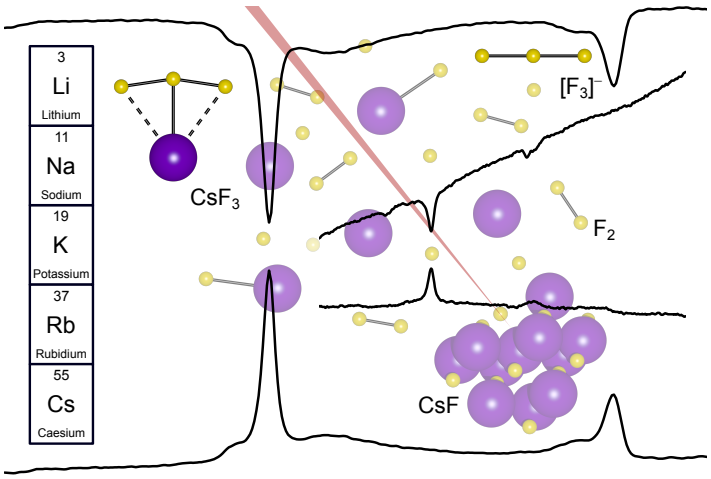


Frenio A. Redeker, Helmut Beckers and Sebastian Riedel*
*RSC Advances* **2015**, *5*, 106568.
https://doi.org/10.1039/c5ra24227d


This work was published during the author's Master's studies and is not part of the doctoral work. However, it has been included in this dissertation as it describes the methodological basis the doctoral work is built on.

**Author Contribution**

Frenio A. Redeker carried out the experiments. Frenio A. Redeker and Sebastian Riedel wrote the manuscript. Sebastian Riedel and Helmut Beckers managed the project and revised the manuscript.

RSC Advances

PAPER

# Investigation of alkali metal polyfluorides by matrix-isolation spectroscopy†

Cite this: *RSC Adv.*, 2015, **5**, 106568

F. A. Redeker, H. Beckers and S. Riedel*

Received 16th November 2015
Accepted 29th November 2015

DOI: 10.1039/c5ra24227d

www.rsc.org/advances

IR laser ablation was used for the systematic matrix-isolation investigation of reaction products of alkali metal fluorides and fluorine. New insights about periodic trends in the reaction behaviour of alkali metals and the formation as well as the photochemistry of alkali metal trifluorides are presented. New bands were found for the antisymmetric stretches of $CsF_3$ and $[F_3]^-$ in solid krypton and nitrogen, and for the combination bands ($\nu_{as} + \nu_s$) of $CsF_3$ and $[F_3]^-$ in solid krypton and argon.

## Introduction

The idea of polyhalide anions has been around since 1817 (ref. 1) and the first crystal structure of a polyhalide salt ($NH_4I_3$) was solved in 1935.[2] Since then and especially in the last 20 years, a large number of polyhalogen anions has been explored.[3] Polyhalides and trihalides ($[X_3]^-$ with X = Cl, Br, I) in particular are of practical use in the fields of organic synthesis,[4,5] superconductivity[6] and polymer science.[7] Some polybromides as well as iodine–chlorine interhalogenides form ionic liquids[8] and are therefore interesting with respect to possible electrochemical applications.

Iodine and bromine compounds dominate the field of polyhalogen anions, while only two polychlorides $[Cl_3]^-$ and $[Cl_3\cdots Cl_2]^-$ have been structurally characterized. Very recently a 2D structure of a polychloride network has been discovered.[9] Beyond these heavier polyhalides which have been characterized by single crystal X-ray diffraction the characterization of polyfluorides is so far only possible in the gas phase or under cryogenic conditions in rare gas matrices. So far, only two polyfluorides, the trifluoride $[F_3]^-$ and the pentafluoride $[F_5]^-$, have been prepared and characterized. The $[F_3]^-$ was first observed as an ion pair complex $MF_3$ (M = K, Rb, Cs) under cryogenic conditions in solid argon.[10–12] An isolated $[F_3]^-$ anion was for the first time observed in the gas phase by mass spectrometry[13,14] and later found to be formed during condensation from a plasma of laser ablated metals and fluorine at 4 K in solid neon and argon.[15] While $[F_4]^{2-}$ has not been observed, yet, $[F_5]^-$ was very recently isolated in neon matrices at 4 K.[12]

As mentioned earlier the polyfluorides can be prepared (a) by thermal evaporation of alkali metal fluorides like CsF, RbF, (b) from the neat metal like potassium using a Knudsen cell, or (c) by laser ablation of neat metals. Both latter techniques need an excess of elemental fluorine. The first technique is not only difficult to implement, it does not allow for the formation of free $F^-$ either, as the energy provided by the Knudsen cell is not high enough.

Therefore only ion-paired complexes can be observed while the second method leads to the formation of free polyfluorides like $[F_3]^-$ and $[F_5]^-$.

In the present investigation we successfully and for the first time used the laser-ablation technique for the ablation of salts. Our setup was using a pulsed focused IR laser for the vaporisation of alkali metal fluorides, as it provides enough energy for the formation of free $F^-$ and therefore isolated polyfluoride monoanions. This method turned out in general to be a suitable and easy to implement method for the ablation of salts into the gas phase. These experiments revealed new insights about matrix isolated alkali metal polyfluorides of the whole alkali metal series and the free polyfluoride $[F_3]^-$, which are herein discussed and reported.

## Results and discussion

In separate matrix-isolation experiments the alkali metal fluorides from LiF to CsF were ablated using a pulsed focused IR laser. During the ablation a mixture of 6% fluorine in neon was passed into the matrix chamber. The reaction products of ablated material and fluorine were deposited on the matrix window and characterized by IR spectroscopy. For lithium and sodium fluoride no reaction products could be observed in the spectral range between 500–4000 $cm^{-1}$, while for potassium, rubidium and caesium fluoride two bands occurred between 500 and 580 $cm^{-1}$ in neon matrices.

In the present work infrared (IR) laser ablation was applied to vaporize alkali metal fluorides, using a pulsed Nd:YAG laser. Although alkali fluorides are transparent for light of the wavelength $\lambda = 1064$ nm it is indeed possible to use a focused Nd:YAG laser for the IR ablation. The mechanisms that lead to the

*Institut für Chemie und Biochemie – Anorganische Chemie, Freie Universität Berlin, Fabeckstrasse 34-36, 14195 Berlin, Germany. E-mail: s.riedel@fu-berlin.de*

† Electronic supplementary information (ESI) available. See DOI: 10.1039/c5ra24227d

ablation of transparent materials with light of energy lower than the band gap can be explained by two effects.[16,17] First, the band gap can be overcome by a multiphoton excitation. The other phenomena that increase the absorption of transparent materials are impurities and/or crystallographic imperfections, *i.e.* defects which lead to the formation of colour centres. The latter is assumed to be the main driving force as it forms localized electronic states inside the band gap resulting in a resonant enhancement of absorption by several orders of magnitude. Given that the targets used in this work are pellets of previously ground material (see Experimental section), defects might be the leading factor in the observed ablation. Using an optically polished NaF single crystal target did not lead to ablation of sodium fluoride but instead of the aluminium target holder.

Fig. 1 shows transmittance spectra of the reaction products of MF (M = K, Rb, Cs) with fluorine in solid neon. The band at 561 $cm^{-1}$ that appeared in all three spectra could be identified as the antisymmetric stretching vibration ($\nu_{as}$) band of the respective metal trifluoride ion pair $M^+[F_3]^-$ which has already been reported to be formed when vaporized potassium or caesium fluoride react with fluorine.[12]

The weaker band at 524 $cm^{-1}$ that also appeared in all three spectra could be assigned to the antisymmetric stretching vibration ($\nu_{as}$) of the free trifluoride $[F_3]^-$ anion isolated in solid neon. The free trifluoride anion has already been reported to be formed in a similar setup, where transition metals were used as targets for laser ablation. In experiments where alkali fluorides were vaporized in a Knudsen cell, the free trifluoride anion has never been observed so far due to a lack of free fluoride anions in the gas phase. The fact that free $[F_3]^-$ occurs in the present work indicates the presence of free $F^-$ anions in the laser-ablation plasma of the alkali metal fluoride pellets. The band positions and relative intensities of the observed polyfluoride bands are listed in Table 1.

Table 1 Band positions of $\nu_{as}$ in $cm^{-1}$ of free $[F_3]^-$ and ion pairs $MF_3$ (M = Li, Na, K, Rb, Cs) in solid neon

| Alkali Fluoride | $MF_3$ | Intensity[a] | Free $[F_3]^-$ | Intensity[a] |
|---|---|---|---|---|
| LiF[b] | n.o. | n.o. | n.o. | n.o. |
| NaF[b] | n.o. | n.o. | n.o. | n.o. |
| KF | 561.2 | 0.8 | 524.6 | 0.1 |
| RbF | 561.2 | 2.4 | 524.6 | 0.3 |
| CsF | 561.2 | 3.3 | 524.3 | 0.5 |

[a] Intensities obtained by integration of band areas (transmittance) and related to the band intensity observed for $CsF_3$ in argon (see Table 2). [b] n.o.: not observed.

The corresponding difference spectra (b) in Fig. 1 show to what extend the matrix changes when irradiated with light of the wavelength $\lambda$ = 455 nm. Bands pointing upwards indicate depletion of the corresponding molecular species. In all three cases the antisymmetric band of the $M^+[F_3]^-$ (M = K, Rb, Cs) ion pairs as well as the free $[F_3]^-$ anion vanished during irradiation with this blue light. The assumption that $[F_3]^-$ absorbs blue light would suggest a yellow colour for this species. However, it seems more likely that fluorine is cleaved photolytically and the fluorine radicals react with $[F_3]^-$.

Changing the matrix host gas from neon to argon shifts the corresponding bands to lower wavenumbers. Fig. 2 shows the 500–580 $cm^{-1}$ region of the transmittance spectra of the reaction products of IR laser ablated MF (M = Li, Na, K) with fluorine in solid argon. In contrast to the experiments in solid neon, the spectra obtained with LiF and NaF show a band in this area. The band at 510 $cm^{-1}$ that appears in each of the spectra is due to the antisymmetric stretching frequency of the free trifluoride monoanion as reported already in 2010.[15]

The ion pair $M^+[F_3]^-$ is not observed in any of these spectra, although $K^+[F_3]^-$ was observed in neon. The relative intensities

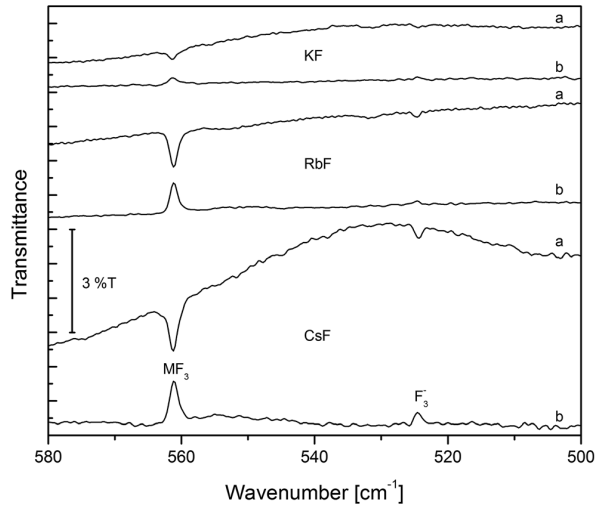


Fig. 1 IR spectra of reaction products of laser ablated KF, RbF and CsF with excess $F_2$ in solid neon at 5 K, (a) transmittance spectra of MF + $F_2$ (6% in solid neon), (b) difference spectra after irradiation with $\lambda$ = 455 nm.

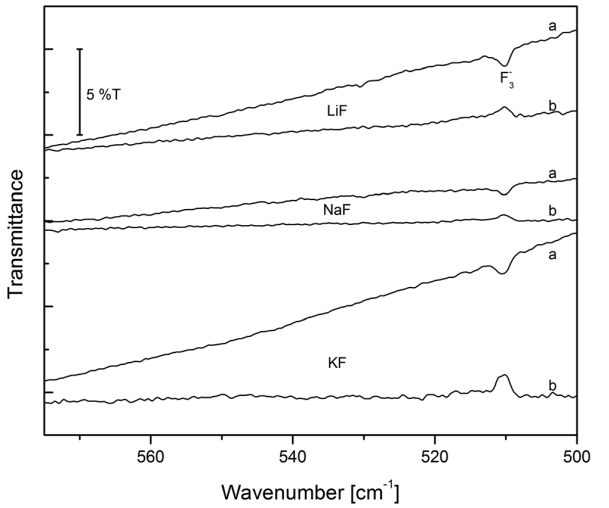


Fig. 2 IR spectra of reaction products of laser ablated LiF, NaF and KF, and $F_2$ in solid argon at 5 K, (a) transmittance spectra of MF + $F_2$ (6% in solid argon), (b) difference spectra after irradiation with $\lambda$ > 220 nm.

displayed in Table 2 are generally higher than those in neon (Table 1), which indicates that the formation of the free $[F_3]^-$ anion is favoured in argon. An explanation, why the ion pair is not formed with lower alkali metals could be that LiF and NaF show stronger coulomb interactions. The formation of the free polyfluorides is then only possible in cases where the cation and anion separation in the gas phase is large enough so that no interaction can occur.

Fig. 3 shows the spectral region 500–580 $cm^{-1}$ of the transmittance spectra of the reaction products of laser ablated rubidium and caesium fluoride with fluorine in solid argon. These spectra show two large bands in this region. The smaller band at 510 $cm^{-1}$ can be assigned to $\nu_{as}$ of $[F_3]^-$, see above. The larger band at around 550 $cm^{-1}$ is known as $\nu_{as}$ of the ion pair $M^+[F_3]^-$ in argon.[10,11] The intense $\nu_{as}(Rb^+[F_3]^-)$ and the even more intense $\nu_{as}(Cs^+[F_3]^-)$ support the assumption that higher alkali metal cations can form more stable ion pairs with $[F_3]^-$ than the lower ones. However, not only more ion pairs were observed for the higher alkali metal fluorides but also larger amounts of free $[F_3]^-$ anions. This can be explained with the decreasing coulomb interaction in the direction of higher alkali metal fluorides allowing for easier formation of free $F^-$ in the plasma, see also the paragraph above.

Table 2 shows the band positions of the antisymmetric vibrations of the observed polyfluorides and their relative intensities obtained by integration of transmittance band areas for the matrix-isolation experiments in solid argon. Both spectra b shown in Fig. 2 and 3 are difference spectra obtained after irradiation with light of a wavelength $\lambda > 220$ nm. In contrast to the experiments in neon, the bands were not easily destroyed by irradiation with blue light ($\lambda = 455$ nm), which supports the hypothesis that the photolysis in neon is due to a secondary effect and could therefore mean that fluorine radicals cannot migrate through the argon matrix as easily as in neon. The disappearance of the bands after irradiation with light of higher frequency is considered to be due to direct photolysis.

As shown above and in agreement with our understanding of chemical bond, the largest amount of polyfluorides have been prepared by laser ablation of caesium fluoride. The matrix-isolation experiments with caesium fluoride in argon yielded such intense bands for the antisymmetric stretching vibrations of the ion pair $Cs^+[F_3]^-$ and free $[F_3]^-$ that combination bands appeared in the area between 890 and 930 $cm^{-1}$. The transmittance spectrum of the reaction products of CsF and $F_2$ (6%) in solid argon as well as the difference spectrum after irradiation ($\lambda = 266$ nm) are shown in Fig. 4, the positions and relative intensities of the bands are listed in Table 3.

The stronger band at 923 $cm^{-1}$ can be assigned to the $\nu_{as} + \nu_s$ combination band of the $Cs^+[F_3]^-$ ion pair as this is in good agreement with the sum of the fundamentals $\nu_{as} + \nu_s = 549.9 + 389 = 938.9$ $cm^{-1}$. The previously reported Raman band assigned by Ault *et al.* to the $\nu_s$ band at 461 $cm^{-1}$ has to be reassigned to the weaker band shown in the same spectrum at 389 $cm^{-1}$,[11] which agrees very well with our predicted band. The

Table 2 Band positions of $\nu_{as}$ in $cm^{-1}$ of free $[F_3]^-$ and ion pairs $MF_3$ (M = Li, Na, K, Rb, Cs) in solid argon

| Alkali fluoride | $MF_3$ | Intensity[a] | Free $[F_3]^-$ | Intensity[a] |
|---|---|---|---|---|
| LiF[b] | n.o. | n.o. | 510.2 | 2.4 |
| NaF[b] | n.o. | n.o. | 510.3 | 1.3 |
| KF | n.o. | n.o. | 510.4 | 2.8 |
| RbF | 549.2 | 17.9 | 510.7 | 5.3 |
| CsF | 549.9 | 100.0 | 510.6 | 25.5 |

[a] Intensities obtained by integration of band areas (transmittance) and related to the band intensity observed for $CsF_3$ in argon. [b] n.o.: not observed.

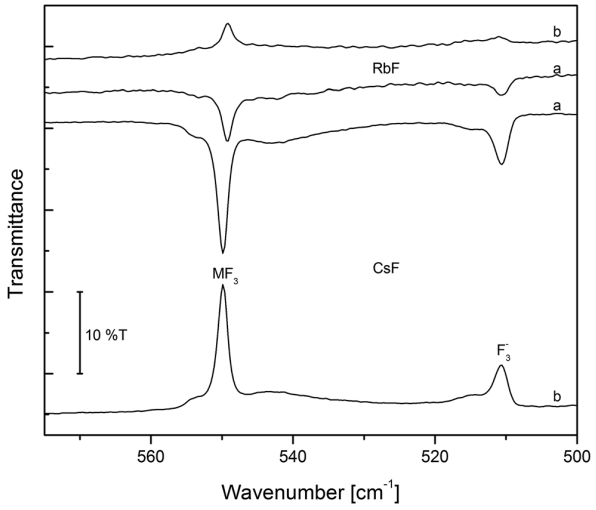


Fig. 3 IR spectra of reaction products of laser ablated RbF and CsF and $F_2$ in solid argon at 5 K, (a) transmittance spectra of MF + $F_2$ (6% in solid argon), (b) difference spectra after irradiation with $\lambda > 220$ nm.

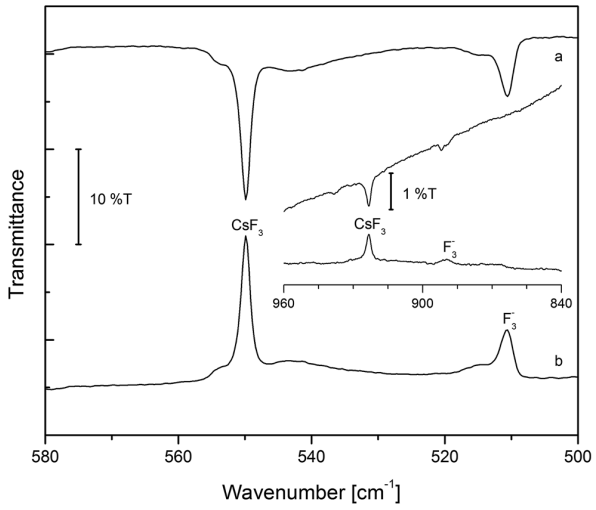


Fig. 4 IR spectra of reaction products of laser ablated CsF and $F_2$ in solid argon at 5 K, (a) transmittance spectrum of CsF + $F_2$ (6% in solid argon), (b) difference spectrum after irradiation with $\lambda = 266$ nm.

Table 3 Band positions of $\nu_{as}$ and of the combination band $\nu_{as} + \nu_s$ in $cm^{-1}$ of the ion pair $CsF_3$ and free $[F_3]^-$ in solid argon, krypton and calculated values

| Vibration | $CsF_3$ | Intensity[a] | Free $[F_3]^-$ | Intensity[a] |
|---|---|---|---|---|
| **Argon** | | | | |
| $\nu_{as}$ | 549.9 | 100.0 | 510.6 | 25.5 |
| $\nu_s$ | 389[b] | — | 396 ± 5[c] | — |
| $\nu_{as} + \nu_s$ | 923.4 | 2.5 | 892.0 | 0.5 |
| **Krypton** | | | | |
| $\nu_{as}$ | 546.5 | 107.6 | 511.7 + 508.8 | 27.8 |
| $\nu_s$ | 388 ± 5[c] | — | 394 ± 5[c] | — |
| $\nu_{as} + \nu_s$ | 919.0 | 2.0 | 888.8 | 0.8 |
| **Nitrogen** | | | | |
| $\nu_{as}$ | 551.0 | 17.2 | 517.3 | 2.4 |
| **Calculated** | | | | |
| $\nu_{as}$ | 568.2[d] | — | 523.4[e] | — |
| $\nu_s$ | 388.2[d] | — | 397.0[e] | — |

[a] Intensities obtained by integration of band areas (transmittance) and related to the band intensity observed for $CsF_3$ in argon. [b] Raman band.[11] [c] Predicted from the observed combination band $\nu_{as} + \nu_s$. [d] CCSD(T)(anharm.)/def2-QZVPP.[9] [e] CCSD(T)(anharm.)/aug-cc-pVQZ.[15]

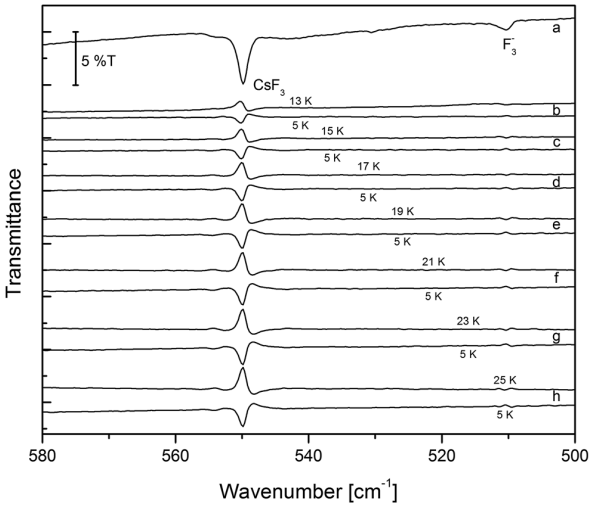


Fig. 5 IR spectra of reaction products of laser ablated CsF and $F_2$ in solid argon, (a) transmittance spectrum of CsF + $F_2$ (6%) in solid argon at 5 K, (b)–(h) difference spectra between spectra recorded at 13 K, 15 K, 17 K, 19 K, 21 K, 23 K and 25 K and spectra recorded at 5 K (bands pointing upwards indicate depletion, bands pointing downwards indicate formation of the corresponding species).

observed combination band is shifted by 15 $cm^{-1}$ towards lower wavenumbers due to anharmonicity. The newly assigned Raman band of $Cs^+[F_3]^-$ is in excellent agreement with the recently calculated value of 388.2 $cm^{-1}$ at the CCSD(T)/def2-QZVPP level.[12] The simultaneous disappearance of the two bands at 550 $cm^{-1}$ and 923 $cm^{-1}$ during irradiation ($\lambda = 266$ nm) is an additional proof for those two bands belonging to the same molecular species, see Fig. 4.

The weaker band at 892 $cm^{-1}$ also disappears after irradiation with light of the wavelength $\lambda = 266$ nm as does the band at 510 $cm^{-1}$. Taking this into account, the band at 892 $cm^{-1}$ can be assigned to the combination band $\nu_{as} + \nu_s$ of the free $[F_3]^-$ anion, especially because of the good correlation of the intensity ratios of the two fundamental bands in comparison with the two combination bands. Based on the newly observed combination band taking the anharmonicity $x_{13}$ into account, the symmetric stretching band $\nu_s$ of the free $[F_3]^-$ anion can be predicted to appear at around $\nu_s = (\nu_{as} + \nu_s) - \nu_{as} + x_{13} = 892.0 - 510.6 + 15 = 396.4$ $cm^{-1}$ which would be consistent with the calculated value of 397.0 $cm^{-1}$ at CCSD(T)/aug-cc-pVQZ level.[15]

Fig. 5 shows transmittance spectra of the reaction products of IR laser ablated CsF with $F_2$ (6%) in solid argon after deposition (a) and difference spectra after annealing to 13 K (b), 15 K (c), 17 K (d), 19 K (e), 21 K (f), 23 K (g), and 25 K (h). Difference spectra at each annealing temperature were obtained by using the preceding low temperature spectrum at 5 K, respectively.

The upwards pointing bands at 550 $cm^{-1}$ in the higher temperature difference spectra (b–h) in Fig. 5 clearly indicate the decomposition of the ion pair $Cs^+[F_3]^-$ at 13–25 K. The difference spectra recorded after recooling to 5 K (b–h) show downwards pointing bands at 550 $cm^{-1}$ which is indicative for a reformation of the ion-pair complex $Cs^+[F_3]^-$ during recooling. This observation suggests that $Cs^+[F_3]^-$ exists in a reversible equilibrium with CsF and $F_2$ at temperatures below 25 K.

$$CsF_3 \underset{5\ K}{\overset{25\ K}{\rightleftharpoons}} CsF + F_2 \quad (1)$$

During annealing small amounts of $F_2$ are constantly withdrawn from the equilibrium which leads to decreasing band intensities in the 5 K spectra. This loss of $F_2$ is probably due to inhomogeneous heating of the matrix window as the measured temperature does not perfectly represent the temperature at any part of the matrix. Annealing at temperatures higher than 25 K lead to complete evaporation of $F_2$ resulting in an irreversible decomposition of the ion pair complex.

We also repeated the annealing experiments in krypton matrices showing the same effects as described above, see Fig. S1 in ESI.† In krypton complete decomposition of $Cs^+[F_3]^-$ starts at 20 K. In Fig. S2† it can be seen that the combination band $\nu_{as} + \nu_s$ at 919 $cm^{-1}$ shows the same reversible thermal behaviour as the $\nu_{as}$ of the $Cs^+[F_3]^-$ in krypton. This supports again our assignment of this band to a combination band. The band shows a small red-shift of 3 $cm^{-1}$ if compared with the argon matrix.

The combination band of $[F_3]^-$ at 889 $cm^{-1}$ appears 3 $cm^{-1}$ lower than the $\nu_{as} + \nu_s$ combination in argon. Using the observed values of $\nu_{as} + \nu_s$ $Cs^+[F_3]^-$ and $\nu_{as} + \nu_s$ $[F_3]^-$ and the respective antisymmetric stretching vibrations in solid krypton, the corresponding symmetric stretching vibrations can be predicted to appear around $\nu_s(CsF_3) = 919.0 - 546.5 + 15 = 387.5$ $cm^{-1}$ and $\nu_s([F_3]^-) = 888.8 - (511.7 + 508.8/2) + 15 = 393.6$ $cm^{-1}$, taking anharmonicity into account. Their positions as well as the predicted Raman bands for the symmetrical stretching modes

in solid krypton are listed in Table 3. Fig. S3† shows the transmittance spectrum of the reaction products of IR laser ablated CsF and $F_2$ (6%) in solid nitrogen. The bands at 551 $cm^{-1}$ and 517 $cm^{-1}$ vanish during irradiation ($\lambda > 220$ nm) and can be assigned to the antisymmetric stretching frequencies of $Cs^+[F_3]^-$ and $[F_3]^-$, respectively. In contrast to the experiments in argon and krypton, but analogue to the experiment with neon, the yields of the polyfluorides were not high enough for combination bands to be observed.

## Conclusions

In the present work the reaction products of laser ablated alkali metal fluorides (M = Li, Na, K, Rb, Cs) with elemental fluorine were investigated under cryogenic conditions in solid neon as well as in solid argon. The experiments in neon showed that the yields of $M^+[F_3]^-$ and free $[F_3]^-$ increase towards higher alkali metal fluorides, as for LiF and NaF these products were not observed at all. The experiments in argon showed no formation of the metal trifluorides for LiF, NaF and KF but a formation of the free trifluoride anion. For RbF and especially CsF large amounts of both trifluoride anions were observed. Again the yields increased towards higher alkali fluorides. In argon, photolysis at $\lambda = 455$ nm was not sufficient. Light of the wavelength $\lambda > 220$ nm was necessary, indicating that migration of fluorine radicals is hindered in argon. Especially the experiments with caesium fluoride yielded new information about the polyfluorides. New bands for the antisymmetric stretches of both molecules were found in krypton and nitrogen and the band positions of the combination vibrations ($\nu_{as} + \nu_s$) were determined for both molecules in krypton and argon. Based on the newly found information it was possible to predict the Raman band positions of the corresponding symmetric stretches. Additionally a reversible decomposition of the ion pair complex $Cs^+[F_3]^-$ was found between 5 and 25 K in solid argon and between 5 and 20 K in solid krypton. The photolysis experiments in solid argon revealed a specific wavelength ($\lambda =$ 266 nm) at which both anions could be photolysed.

Beyond these observations, it should be mentioned, that other metal fluorine species such as the star like $CsF_5$ which has recently been predicted based on quantum-chemical calculations have not been observed in the present work.[18]

## Experimental

The experimental apparatus used for laser ablated alkali metal fluoride reactions with $F_2$ in different host gases during condensation at 5 K using a closed-cycle helium cryostat (Sumitomo Heavy Industries, RDK-205D) inside the vacuum chamber has been described in more detail in our previous works.[19] The alkali metal fluoride samples were rotated in a self-built matrix chamber with a magnetic bearing motor in a distance of 4 cm from the cold window. The laser beam was focused using a plano convex lens with a diameter of 25.4 mm and a focal distance of 125.0 mm. Commercial fluorine (99.8%, Solvay) was purified by trap to trap distillation and photolysis to eliminate all common impurities.[20] The Nd:YAG laser fundamental (Continuum, Minilite II, 1064 nm, 10 Hz repetition rate with 7 ns pulse width) with a pulse energy of up to 50 mJ $cm^{-2}$ was focused onto the alkali metal fluoride targets, which gave an energetic plasma beam reacting with $F_2$ spreading toward the cold CsI window. FTIR spectra were recorded on a Bruker Vertex 70 spectrometer purged with dry air at 0.5 $cm^{-1}$ resolution with 0.5 $cm^{-1}$ accuracy in the band positions. Matrix samples were annealed at different temperatures, and selected samples were subjected to irradiation by a medium pressure mercury arc street lamp with the outer globe removed (>220 nm). Selective irradiation with 455 nm and 266 nm was carried out using a self-made LED and a Nd:YAG laser source with quadrupled frequency, respectively. Potassium fluoride, rubidium fluoride and caesium fluoride were dried *via* heating to 900 °C in a platinum crucible using a muffle furnace. The molten material was then tipped into a bowl of stainless steel and directly transferred into a glovebox and pestled. Lithium and sodium fluoride were used as received. All alkali fluoride targets (LiF, NaF, KF, RbF, CsF) were prepared in a hydraulic lab press. The respective alkali metal fluoride powder was filled into the pressing tool inside a glovebox. After pressing, the tool was opened inside the glovebox to avoid contamination with atmospheric $H_2O$.

## Acknowledgements

Prof. J. Reif from the TU Chemnitz is gratefully acknowledged for fruitful discussions. S. R. thanks the DFG graduate research training group, 1582/2 "*Fluorine as a Key Element*". The authors are grateful to Dr Eicher from the Solvay Fluor GmbH for the generous support with $F_2$ and to Korth Kristalle for the donation of alkali metal fluoride crystals.

## Notes and references

1 J. Pelletier and J. B. Caventou, *Ann. Chim. Phys.*, 1819, 142–177.
2 R. C. Mooney, *Z. Kristallogr.–Cryst. Mater.*, 1935, **90**, 143–150.
3 H. Haller and S. Riedel, *Z. Anorg. Allg. Chem.*, 2014, **640**, 1281–1291.
4 P. J. Stang, *Chem. Rev.*, 1996, **96**, 1123.
5 T. Schlama, K. Gabriel, V. Gouverneur and C. Mioskowski, *Angew. Chem., Int. Ed. Engl.*, 1997, **36**, 2342–2344.
6 J. M. Williams, H. H. Wang, T. J. Emge, U. Geizer, M. A. Beno, P. C. Leung, K. D. Carlson, R. J. Thorn, A. J. Schultz and M. H. Whangbo, *Inorg. Chem.*, 1987, **35**, 51.
7 I. Harada, Y. Furukawa, M. Tasumi, H. Shirakawa and S. Ikeda, *J. Chem. Phys.*, 1980, **73**, 4746–4757.
8 M. Wolff, A. Okrut and C. Feldmann, *Inorg. Chem.*, 2011, **50**, 11683–11694.
9 R. Brückner, H. Haller, S. Steinhauer, C. Müller and S. Riedel, *Angew. Chem., Int. Ed.*, 2015, **54**, 15579–15583; *Angew. Chem.*, 2015, **127**, 15800–15804.
10 B. S. Ault and L. Andrews, *J. Am. Chem. Soc.*, 1976, **98**, 1591–1593.
11 B. S. Ault and L. Andrews, *Inorg. Chem.*, 1977, **16**, 2024–2028.

12 T. Vent-Schmidt, F. Brosi, J. Metzger, T. Schlöder, X. Wang, L. Andrews, C. Müller, H. Beckers and S. Riedel, *Angew. Chem., Int. Ed.*, 2015, **54**, 8279–8283.
13 A. A. Tuinman, A. A. Gakh, R. J. Hinde and R. N. Compton, *J. Am. Chem. Soc.*, 1999, **121**, 8397–8398.
14 A. Artau, K. E. Nizzi, B. T. Hill, L. S. Sunderlin and P. G. Wenthold, *J. Am. Chem. Soc.*, 2000, **122**, 10667–10670.
15 S. Riedel, T. Köchner, X. Wang and L. Andrews, *Inorg. Chem.*, 2010, **49**, 7156–7164.
16 J. Reif, *Opt. Eng.*, 1989, **28**, 1122–1132.
17 M. Henyk, F. Costache and J. Reif, *Appl. Surf. Sci.*, 2002, **197**, 90–95.
18 A. Y. Rogachev, M.-S. Miao, G. Merino and R. Hoffmann, *Angew. Chem., Int. Ed.*, 2015, **54**, 8275–8278.
19 T. Schlöder, T. Vent-Schmidt and S. Riedel, *Angew. Chem., Int. Ed.*, 2012, **51**, 12063–12067.
20 F. Brosi, T. Vent-Schmidt, S. Kieninger, T. Schlöder, H. Beckers and S. Riedel, *Chem.–Eur. J.*, 2015, **21**, 16455–16462.

# Supporting Information

# Investigation of Alkali Metal Polyfluorides by Matrix-Isolation Spectroscopy

Frenio A. Redeker, Helmut Beckers, Sebastian Riedel*

*Institut für Chemie und Biochemie – Anorganische Chemie, Freie Universität Berlin, Fabeckstrasse 34-36, 14195 Berlin, Germany*

B.Sc. Frenio A. Redeker, Dr. habil. Helmut Beckers, Prof. Dr. Sebastian Riedel

E-Mail: s.riedel@fu-berlin.de

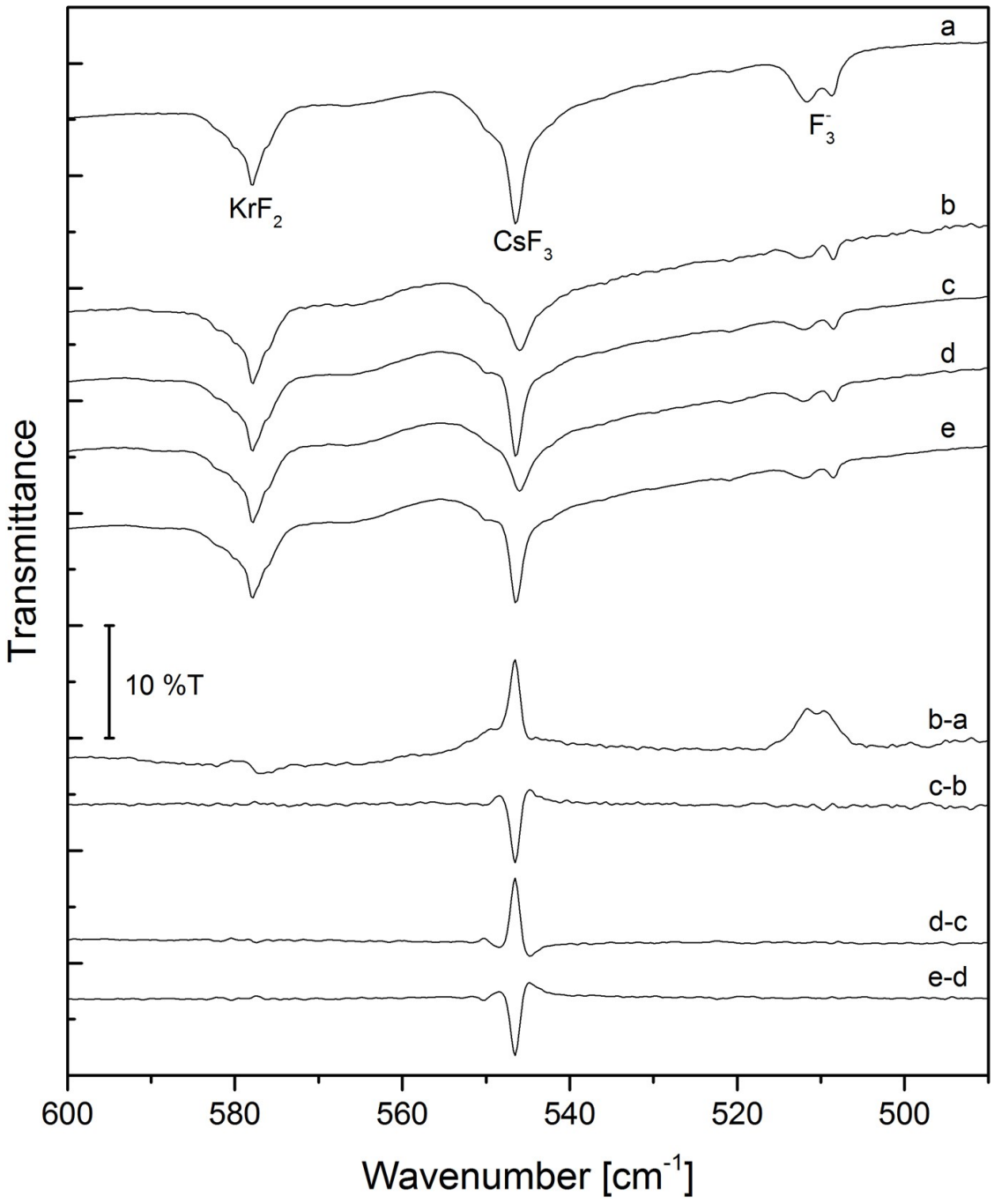


**Figure S1:** IR spectra of reaction products of laser ablated CsF and $F_2$ in solid krypton, a) transmittance spectrum of CsF + $F_2$ (6 %) in solid krypton at 5 K, b) transmittance spectrum after heating to 20 K, c) transmittance spectrum after recooling to 5 K, d) transmittance spectrum after repeated heating to 20 K, e) transmittance spectrum after repeated cooling to 5 K, y-x) difference spectra - bands pointing upwards indicate depletion, bands pointing downwards indicate formation of the corresponding species.

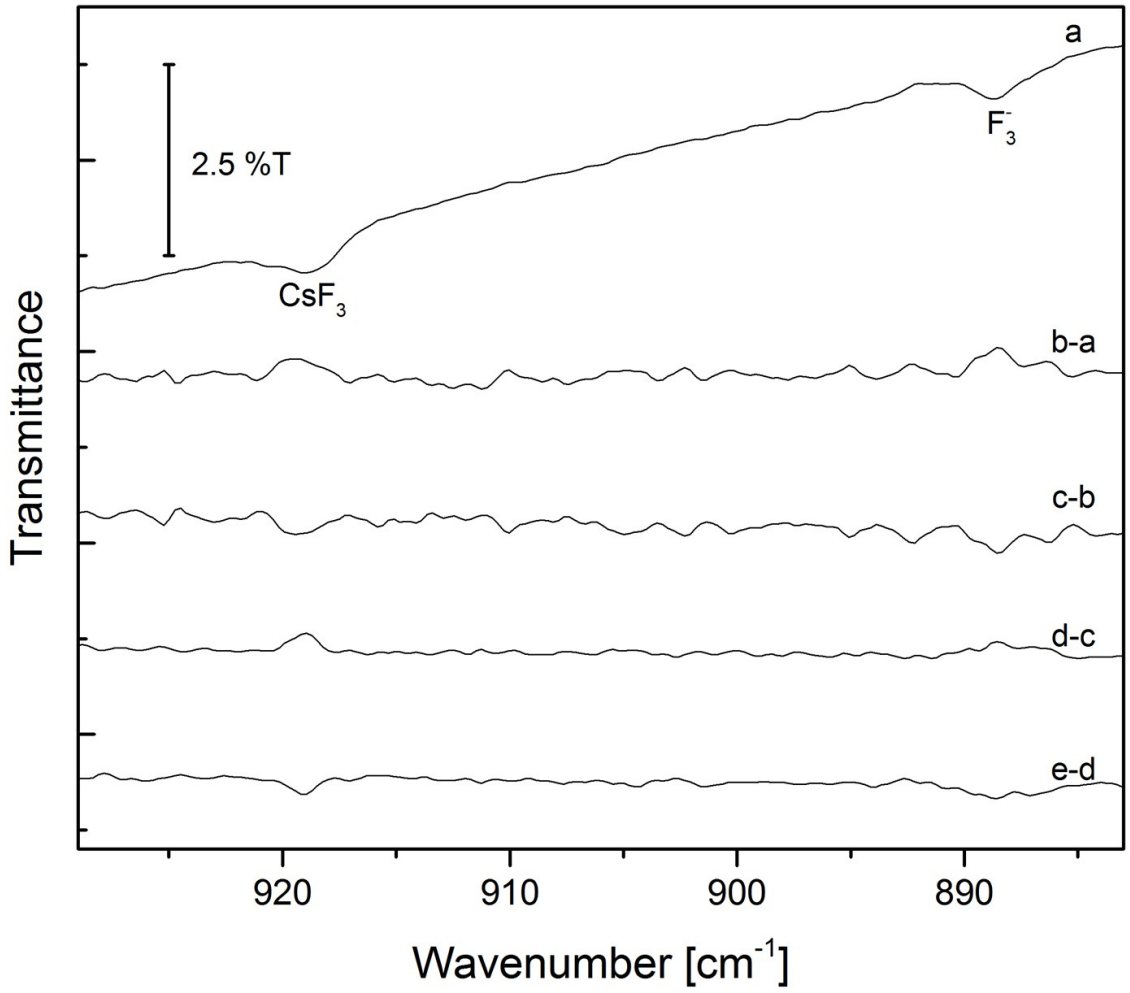


**Figure S2:** Combination bands in the region from 880 to 930 $cm^{-1}$ of the spectra displayed in S1.

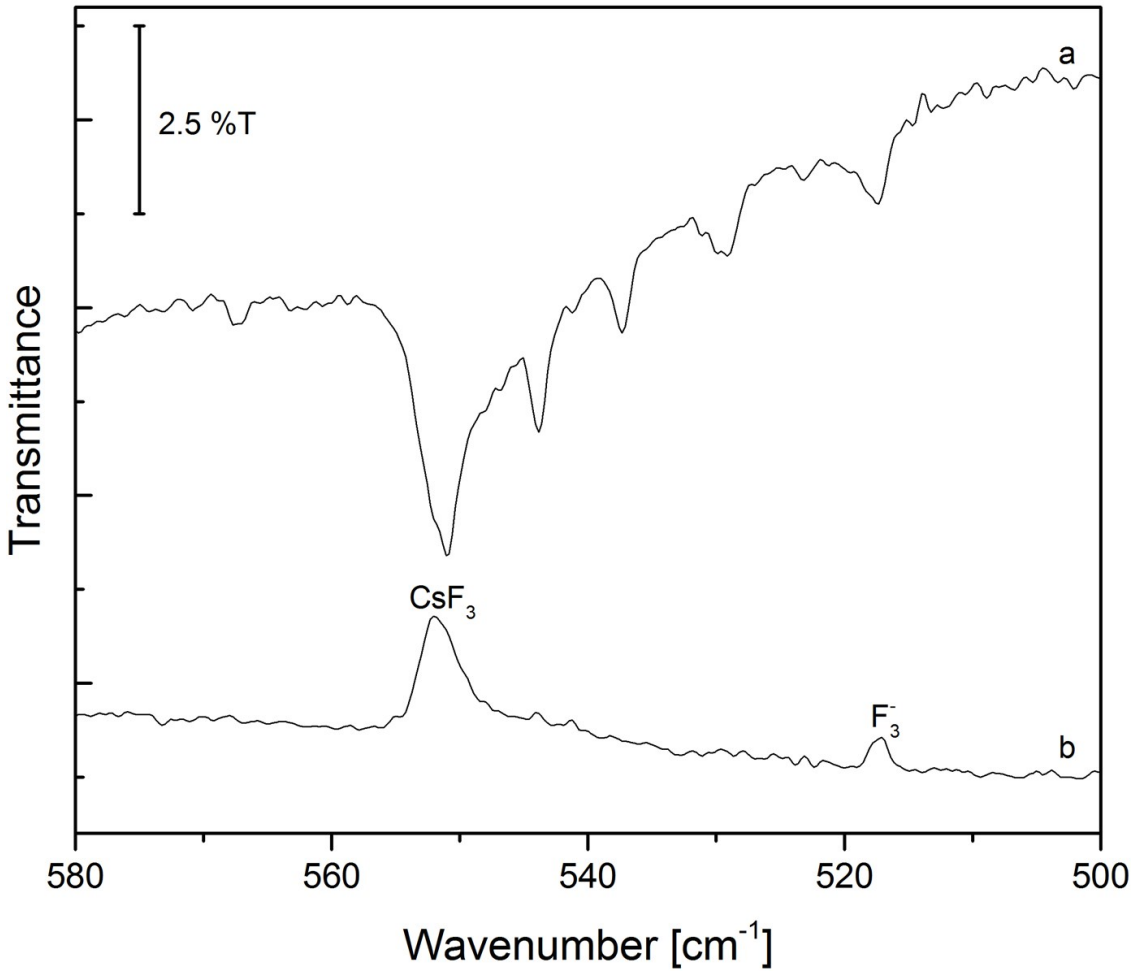


**Figure S3:** IR spectra of reaction products of laser ablated CsF and $F_2$ in solid nitrogen at 5 K, a) transmittance spectrum of CsF + $F_2$ (6 %) in solid nitrogen, b) difference spectrum after irradiation with λ > 220 nm.

## 4.2 Matrix-Isolation and Comparative Far-IR Investigation of Free Linear $Cl_3^-$ and a Series of Alkali Trichlorides

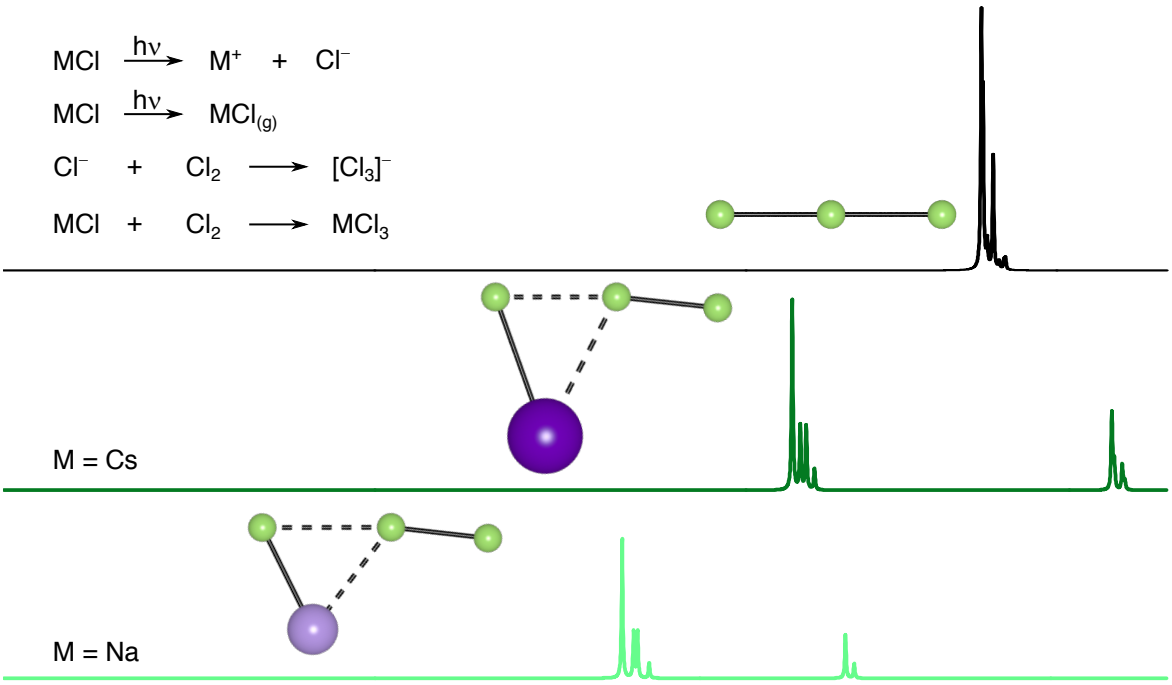


Frenio A. Redeker, Helmut Beckers and Sebastian Riedel*
*Chemical Communications* **2017**, *53*, 12958.
https://doi.org/10.1039/c7cc08290h


**Author Contribution**

Frenio A. Redeker carried out the experiments and wrote the manuscript. Sebastian Riedel and Helmut Beckers managed the project and revised the manuscript.

## 4.3 Theoretical Investigation of the Structures, Stabilities and Vibrational Properties of Triatomic Interhalide Anions and their Alkali Ion Pairs

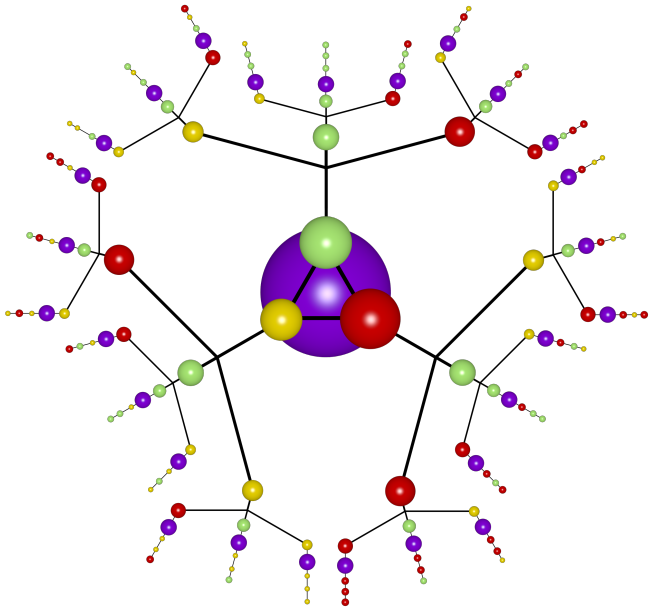

Frenio A. Redeker, Alexej Kropman, Carsten Müller, Sarah E. Zewge, Helmut Beckers, Beate Paulus* and Sebastian Riedel*
*Journal of Fluorine Chemistry* **2018**, *216*, 81.
https://doi.org/10.1016/j.jfluchem.2018.10.007


**Author Contribution**

Frenio A. Redeker designed the project, wrote most of the manuscript and did calculations. Alexej Kropman carried out most of the calculations on alkali interhalides under the supervision of Frenio A. Redeker. Carsten Müller wrote the part about free trihalides, Sarah E. Zewge did the calculations on free trihalides under the supervision of Carsten Müller. Helmut Beckers revised the manuscript, Sebastian Riedel and Beate Paulus managed the project and revised the manuscript.

## 4.4 IR-Laser Ablation of KCN: A Surprisingly Simple Route to Polynitrogen and Polycarbon Species

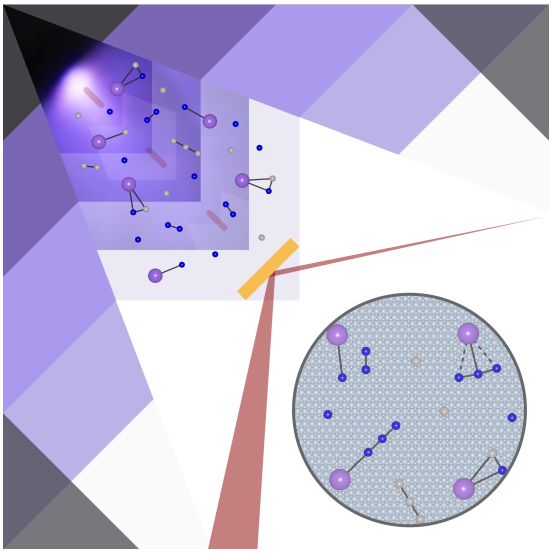

Frenio A. Redeker, Helmut Beckers and Sebastian Riedel*
*Chemistry – A European Journal* **2019**, accepted.
https://doi.org/10.1002/chem.201905103


**Author Contribution**

Frenio A. Redeker carried out the experiments and wrote the manuscript. Sebastian Riedel and Helmut Beckers managed the project and revised the manuscript.

## 4.5 Investigation of Molecular Alkali Tetrafluorido Aurates by Matrix-Isolation Spectroscopy

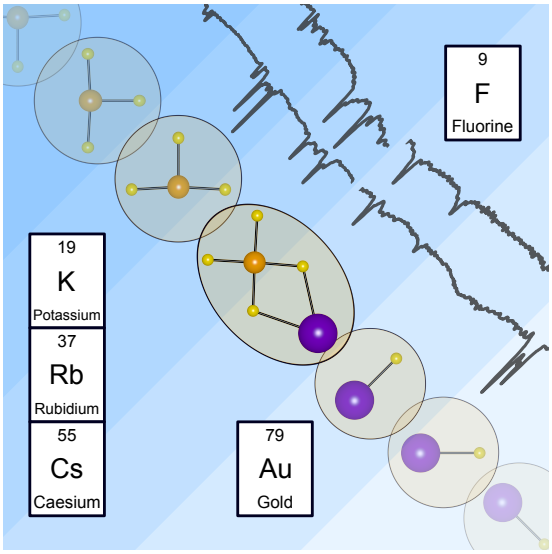


Frenio A. Redeker, Mathias A. Ellwanger, Helmut Beckers and Sebastian Riedel*
*Chemistry – A European Journal* **2019**, 25, 15059.
https://doi.org/10.1002/chem.201904335


**Author Contribution**

Frenio A. Redeker carried out the experiments and wrote the manuscript. Mathias A. Ellwanger synthesized the precursors and revised the manuscript. Sebastian Riedel and Helmut Beckers managed the project and revised the manuscript.

# 5 Conclusion

A method for the efficient vaporization of IR-transparent salts and production of free halide ions ($X^-$, X = F, Cl) was developed by applying IR-laser ablation to pellets of alkali halides MX. The formation of $X^-$ during laser ablation of MX is proven by the formation of free polyhalogen anions like $X_3^-$.

Due to the high product yields provided by that method it was possible to study the combination bands $\nu_3 + \nu_1$ of the free $F_3^-$ ion experimentally and for all its alkali ion pairs (M = K-Cs) after co-deposition of laser-ablated MF in solid neon matrices at 6 K. The fact that combination bands of $MF_3$ could be observed using laser ablation of MF with low deposition times shows that this method is a significant improvement to the conventional Knudsen effusion in which no free ions can be produced at all. Those combination bands allowed for a prediction of the lower limits of the unobserved (IR-inactive) symmetric stretches ($\nu_1$) of $F_3^-$, $KF_3$, $RbF_3$, and $CsF_3$ in solid neon. Furthermore, the previously claimed $F_5^-$ species could be studied in more detail as it is also produced in extraordinary high yields by co-deposition of laser ablated alkali fluorides (MF) with difluorine ($F_2$) in solid neon. New insights could be gained about the formation of the challenging $F_5^-$ system with different alkali halides and about its photo chemistry.

With the same method used for the alkali fluorides, a sequence of alkali trichlorides $MCl_3$ with M = Na, K, Rb, and Cs could be isolated in solid neon, and the free $Cl_3^-$ ion isolated in solid neon and argon was IR spectroscopically characterized for the first time. The $\nu_3$ stretches of free $Cl_3^-$ of 252 $cm^{-1}$ in both neon and argon strongly support the assignment by Pimentel of a band at 375 $cm^{-1}$ in solid krypton to the $Cl_3$ radical, which had previously been called in doubt. The experimental results obtained for the alkali ion pairs of $Cl_3^-$ in combination with high-level quantum-chemical calculations allowed for an explanation of some unexpected structural and spectral trends in the series of the alkali trichlorides.

In a subsequent theoretical study the stability of trihalides from various combinations of halides and dihalogens was systematically investigated. The structures and vibrational properties of the alkali trihalides were theoretically characterized. One especially important result of that study is that alkali trifluoride ion pairs $MF_3$ are the only alkali trihalides with $C_{2v}$ symmetry. All other alkali trihalides can be described as adducts of alkali halides with dihalogens (e. g. $NaCl\cdots Cl_2$) having $C_s$ symmetry. This insight made it possible to reassign some IR bands that were previously assigned to non-existing species.

The laser-ablation method used for MF, MCl was also applied to KCN. While that route was found to be not suitable for the generation of free $CN^-$ ions, this method very efficiently

produces polycarbon and polynitrogen species like $C_3$, $C_3^-$, $N_3$, and $N_3^-$ which were studied in solid neon, argon, and dinitrogen $N_2$ matrices. Furthermore, it led to the first spectroscopic observation of a $C_{2v}$ symmetric $KC_3$ and two molecular $C_{2v}$ and $C_{\infty v}$ symmetric $KN_3$ isomers which are not accessible by any other method. The experiments further yielded evidence for the intermediary formation of potassium nitrene, KN, which is a potential interstellar species of interest.

Finally, it could be shown that the pulsed laser deposition method can be applied to salt mixtures, $MF/AuF_3$, to yield molecular alkali tetrafluorido aurates ($MAuF_4$) after isolation in an excess of neon at 6 K, which were IR spectroscopically characterized for the first time. The mixture $MF/AuF_3$ also yielded IR spectra of molecular $AuF_3$ and an especially nicely resolved spectrum of its dimer $Au_2F_6$, isolated in solid noble gases.

# 6 References


[1] K. Sonnenberg, L. Mann, F. A. Redeker, B. Schmidt, S. Riedel, *Angew. Chem. Int. Ed.* **2019**, 10.1002/anie.201903197R1; K. Sonnenberg, L. Mann, F. A. Redeker, B. Schmidt, S. Riedel, *Angew. Chem.* **2019**, 10.1002/ange.201903197R1.

[2] G. Cavallo, P. Metrangolo, R. Milani, T. Pilati, A. Priimagi, G. Resnati, G. Terraneo, *Chem. Rev.* **2016**, *116*, 2478.

[3] R. K. Brückner, PhD thesis, Freie Universität Berlin, **2016**.

[4] A. Yao, F. Qu, Y. Liu, G. Qu, H. Lin, S. Hu, X. Wang, T. Chu, *Dalton Trans.* **2019**, *48*, 16249.

[5] J. Li, B. E. Bursten, L. Andrews, C. J. Marsden, *J. Am. Chem. Soc.* **2004**, *126*, 3424.

[6] D. Forney, M. E. Jacox, W. E. Thompson, *J. Mol. Spec.* **1993**, *157*, 479.

[7] F. Brosi, T. Vent-Schmidt, S. Kieninger, T. Schloeder, H. Beckers, S. Riedel, *Chem. Eur. J.* **2015**, *21*, 16455.

[8] W. F. Howard, L. Andrews, *J. Am. Chem. Soc.* **1973**, *95*, 3045.

[9] E. S. Prochaska, B. S. Ault, L. Andrews, *Inorg. Chem.* **1977**, *16*, 2021.

[10] L. B. Knight Jr., J. T. Petty, S. T. Cobranchi, D. Feller, E. R. Davidson, *J.Chem. Phys.* **1988**, *88*, 3441.

[11] H. Joly, J. Howard, *J. Phys. Chem. A* **1997**, *101*, 2817.

[12] L. B. Knight Jr., B. W. Gregory, S. T. Cobranchi, D. Feller, E. R. Davidson, *J. Am. Chem. Soc.* **1987**, *109*, 3521.

[13] T. R. Burkholder, L. Andrews, *J. Chem. Phys.* **1991**, *95*, 8697.

[14] V. Bondybey, J. English, *Chem. Phys. Lett.* **1984**, *111*, 195.

[15] M. Rasanen, J. Y. Liu, T. Dzugan, V. Bondybey, *Chem. Phys. Lett.* **1987**, *142*, 308.

[16] V. Bondybay, *Chemistry and Physics of Matrix Isolated Species*, (Eds.: L. Andrews, M. Moskovits), North-Holland, **1989**, p. 130.

[17] V. Bondbey, *Science* **1985**, *227*, 125.

[18] W. Reents, V. Bondybey, *Chem. Phys. Lett.* **1986**, *125*, 324.

[19] L. Shao, L. Zhang, M. Chen, H. Lu, M. Zhou, *Chem. Phys. Lett.* **2001**, *343*, 178.

[20] L. Andrews, P. Hassanzadeh, T. R. Burkholder, J. Martin, *J. Chem. Phys.* **1993**, *98*, 922.

[21] R. Onaka, A. Fukuda, A. Ejiri, *J. Phy. Soc. Japan* **1961**, *16*, 340.

[22] D. Roessler, W. Walker, *J. Phys. Chem. Solids* **1967**, *28*, 1507.

[23] J. Eby, K. Teegarden, D. Dutton, *Phys. Rev.* **1959**, *116*, 1099.

[24] D. Roessler, H. Lempka, *Brit. J. Appl. Phys.* **1966**, *17*, 1553.

[25] J. Reif, *Opt. Eng.* **1989**, *28*, 281122.

[26] M. Henyk, F. Costache, J. Reif, *App. Surf. Sci.* **2002**, *197*, 90.

[27] N. Itoh, K. Hattori, Y. Nakai, J. Kanasaki, A. Okano, R. F. Haglund in *Laser Ablation Mechanisms and Applications*, (Eds.: J. C. Miller, R. F. Haglund Jr.), Springer, **1991**, pp. 217–218.

[28] TURBOMOLE V7.3 **2018**, a development of University of Karlsruhe and Forschungszentrum Karlsruhe GmbH, 1989-2007, TURBOMOLE GmbH, since 2007; available from `http://www.turbomole.com`.

[29] H.-J. Werner, P. J. Knowles, G. Knizia, F. R. Manby, M. Schütz, P. Celani, W. Györffy, D. Kats, T. Korona, R. Lindh, A. Mitrushenkov, G. Rauhut, K. R. Shamasundar, T. B. Adler, R. D. Amos, S. J. Bennie, A. Bernhardsson, A. Berning, D. L. Cooper, M. J. O. Deegan, A. J. Dobbyn, F. Eckert, E. Goll, C. Hampel, A. Hesselmann, G. Hetzer, T. Hrenar, G. Jansen, C. Köppl, S. J. R. Lee, Y. Liu, A. W. Lloyd, Q. Ma, R. A. Mata, A. J. May, S. J. McNicholas, W. Meyer, T. F. Miller III, M. E. Mura, A. Nicklass, D. P. O'Neill, P. Palmieri, D. Peng, K. Pflüger, R. Pitzer, M. Reiher, T. Shiozaki, H. Stoll, A. J. Stone, R. Tarroni, T. Thorsteinsson, M. Wang, M. Welborn, MOLPRO, version 2019.2, a package of ab initio programs, see `https://www.molpro.net`, Cardiff, UK, **2019**.

[30] F. Neese, *WIREs Comput. Mol. Sci.* **2012**, *2*, 73.

[31] F. Neese, *WIREs Comput. Mol. Sci.* **2018**, *8*, e1327.

[32] A. D. Becke, *J. Chem. Phys.* **1993**, *98*, 5648.

[33] C. Lee, W. Yang, R. G. Parr, *Phys. Rev. B* **1988**, *37*, 785.

[34] S. Vosko, L. Wilk, M. Nusair, *Can. J. Phys.* **1980**, *58*, 1200.

[35] P. Stephens, F. Devlin, C. Chabalowski, M. J. Frisch, *J. Phys. Chem.* **1994**, *98*, 11623.

[36] J. P. Perdew, *Phys. Rev. B* **1986**, *33*, 8822.

[37] A. D. Becke, *Phys. Rev. A* **1988**, *38*, 3098.

[38] S. Grimme, *J. Chem. Phys.* **2003**, *118*, 9095.

[39] J. Pelletier, J. B. Caventou, *Ann. Chim. Phys.* **1819**, 142.

[40] S. Jörgensen, *J. F. Prakt. Chem.* **1870**, *2*, 347.

[41] R. Mooney, *Z. Kristallogr.* **1935**, *90*, 143.

[42] P. H. Svensson, L. Kloo, *Chem. Rev.* **2003**, *103*, 1649.

[43] L. Kloo in *Comprehensive Inorganic Chemistry II, From Elements to Applications*, (Eds.: J. Reedijk, K. Poeppelmeier), Elsevier, **2013**, p. 233.

[44] F. D. Chattaway, G. Hoyle, *J. Chem. Soc. Trans.* **1923**, *123*, 654.

[45] M. Groessl, Z. Fei, P. J. Dyson, S. A. Katsyuba, K. L. Vikse, J. S. McIndoe, *Inorg. Chem.* **2011**, *50*, 9728.

[46] H. Haller, J. Schröder, S. Riedel, *Angew. Chem. Int. Ed.* **2013**, *52*, 4937; H. Haller, J. Schröder, S. Riedel, *Angew. Chem.* **2013**, *125*, 5037.

[47] K. Sonnenberg, P. Pröhm, N. Schwarze, C. Müller, H. Beckers, S. Riedel, *Angew. Chem. Int. Ed.* **2018**, *57*, 9136; K. Sonnenberg, P. Pröhm, N. Schwarze, C. Müller, H. Beckers, S. Riedel, *Angew. Chem.* **2018**, *130*, 9274.

[48] B. Schmidt, K. Sonnenberg, H. Beckers, S. Steinhauer, S. Riedel, *Angew. Chem. Int. Ed.* **2018**, *57*, 9141; B. Schmidt, K. Sonnenberg, H. Beckers, S. Steinhauer, S. Riedel, *Angew. Chem.* **2018**, *130*, 9279.

[49] H. Haller, S. Riedel, *Z. Anorg. Allg. Chem.* **2014**, *640*, 1281.

[50] H. Bode, *Naturwissenschaften* **1950**, *37*, 477.

[51] H. Bode, E. Klesper, *Z. Anorg. Allg. Chem.* **1952**, *267*, 97.

[52] H. Bode, E. Klesper, *Z. Anorg. Allg. Chem.* **1961**, *313*, 161.

[53] L. Asprey, J. L. Margrave, M. E. Silverthorn, *J. Am. Chem. Soc.* **1961**, *83*, 2955.

[54] B. S. Ault, L. Andrews, *J. Am. Chem. Soc.* **1976**, *98*, 1591.

[55] B. S. Ault, L. Andrews, *Inorg. Chem.* **1977**, *16*, 2024.

[56] A. A. Tuinman, A. A. Gakh, R. J. Hinde, R. N. Compton, *J. Am. Chem. Soc.* **1999**, *121*, 8397.

[57] A. Artau, K. E. Nizzi, B. T. Hill, L. S. Sunderlin, P. G. Wenthold, *J. Am. Chem. Soc.* **2000**, *122*, 10667.

[58] S. Riedel, T. Köchner, X. Wang, L. Andrews, *Inorg. chem.* **2010**, *49*, 7156.

[59] T. Vent-Schmidt, F. Brosi, J. Metzger, T. Schlöder, X. Wang, L. Andrews, C. Müller, H. Beckers, S. Riedel, *Angew. Chem. Int. Ed.* **2015**, *54*, 8279; T. Vent-Schmidt, F. Brosi, J. Metzger, T. Schlöder, X. Wang, L. Andrews, C. Müller, H. Beckers, S. Riedel, *Angew. Chem.* **2015**, *127*, 8397.

[60] P. A. Cahill, C. E. Dykstra, J. Martin, *J. Am. Chem. Soc.* **1985**, *107*, 6359.

[61] C. S. Ewig, J. R. Van Wazer, *J. Am. Chem. Soc.* **1990**, *112*, 109.

[62] G. L. Heard, C. J. Marsden, G. E. Scuseria, *J. Phys. Chem.* **1992**, *96*, 4359.

[63] T. Kar, E. S. Marcos, *Chem. Phys. Lett.* **1992**, *192*, 14.

[64] T. G. Wright, E. P. Lee, *Mol. Phys.* **1993**, *79*, 995.

[65] N. O. Malcolm, J. J. McDouall, *J. Phys. Chem.* **1996**, *100*, 10131.

[66] F. Mota, J. J. Novoa, *J. Chem. Phys.* **1996**, *105*, 8777.

[67] D. J. Tozer, P. Carlos, *Mol. Phys.* **1997**, *90*, 515.

[68] J. Czernek, O. Zivny, *J. Chem. Phys.* **2008**, *129*, 194305.

[69] B. Braida, P. C. Hiberty, *J. Phys. Chem. A* **2008**, *112*, 13045.

[70] Z. Sun, H. F. Schaefer, *Phys. Chem. Chem. Phys.* **2018**, *20*, 18986.

[71] V. P. Oliveira, E. Kraka, F. B. Machado, *Inorg. Chem.* **2019**, *58*, 14777.

[72] F. Redeker, H. Beckers, S. Riedel, *RSC Adv.* **2015**, *5*, 106568.

[73] L. Andrews, X. Wang, *Phys. Chem. Chem. Phys.* **2018**, *20*, 23378.

[74] G. C. Pimentel, *J. Chem. Phys.* **1951**, *19*, 446.

[75] R. J. Hach, R. Rundle, *J. Am. Chem. Soc.* **1951**, *73*, 4321.

[76] G. A. Landrum, N. Goldberg, R. Hoffmann, *Dalton Trans.* **1997**, 3605.

[77] C. Wang, D. Danovich, S. Shaik, Y. Mo, *Chem. Eur. J.* **2017**, *23*, 8719.

[78] L. Y. Nelson, G. C. Pimentel, *J. Chem. Phys.* **1967**, *47*, 3671.

[79] B. S. Ault, L. Andrews, *J. Am. Chem. Soc.* **1975**, *97*, 3824.

[80] B. S. Ault, L. Andrews, *J. Chem. Phys.* **1976**, *64*, 4853.

[81] C. A. Wight, B. S. Ault, L. Andrews, *J. Chem. Phys.* **1976**, *65*, 1244.

[82] K. S. Thanthiriwatte, J. M. Spruell, D. A. Dixon, K. O. Christe, H. D. B. Jenkins, *Inorg. Chem.* **2014**, *53*, 8136.

[83] Z. Sun, K. B. Moore III, J. G. Hill, K. A. Peterson, H. F. Schaefer III, R. Hoffmann, *J. Phys. Chem. B* **2017**, *122*, 3339.

[84] R. Brückner, H. Haller, S. Steinhauer, C. Müller, S. Riedel, *Angew. Chem. Int. Ed.* **2015**, *54*, 15579; R. Brückner, H. Haller, S. Steinhauer, C. Müller, S. Riedel, *Angew. Chem.* **2015**, *127*, 15800.

[85] J. Evans, G. Y.-S. Lo, *J. Chem. Phys.* **1966**, *44*, 3638.

[86] M. P. Bogaard, J. Peterson, A. D. Rae, *Acta Cryst. B* **1981**, *37*, 1357.

[87] T. Chivers, J. Richardson, N. Smith, *Inorg. Chem.* **1985**, *24*, 2453.

[88] R. T. Boeré, A. W. Cordes, R. T. Oakley, R. W. Reed, *J. Chem. Soc. Chem. Commun.* **1985**, 655.

[89] M. Jansen, S. Strojek, *Z. Naturforsch.* **1995**, *50b*, 1171.

[90] R. Brückner, H. Haller, M. Ellwanger, S. Riedel, *Chem. Eur. J.* **2012**, *18*, 5741.

[91] T. Keilhack, MA thesis, Freie Universität Berlin, **2019**.

[92] R. W. Wyckoff, *J. Am. Chem. Soc.* **1920**, *42*, 1100.

[93] R. M. Bozorth, L. Pauling, *J. Am. Chem. Soc.* **1925**, *47*, 1561.

[94] R. Mooney, *Z. Kristallogr.* **1938**, *98*, 324.

[95] R. Mooney, *Z. Kristallogr.* **1939**, *100*, 519.

[96] G. J. Visser, A. Vos, *Acta Cryst.* **1964**, *17*, 1336.

[97] G. L. Breneman, R. D. Willet, *Acta Cryst.* **1967**, *23*, 334.

[98] J. Davies, E. Nunn, *J. Chem. Soc. D Chem. Commun.* **1969**, 1374a.

[99] W. Gabes, K. Olie, *Cryst. Struct. Comm.* **1974**, *3*, 753.

[100] W. B. Person, G. R. Anderson, J. N. Fordemwalt, H. Stammreich, R. Forneris, *J. Chem. Phys.* **1961**, *35*, 908.

[101] M. Gorlov, H. Pettersson, A. Hagfeldt, L. Kloo, *Inorg. Chem.* **2007**, *46*, 3566.

[102] K. Christe, J. Guertin, *Inorg. Chem.* **1965**, *4*, 905.

[103] K. O. Christe, J. P. Guertin, *Inorg. Chem.* **1965**, *4*, 1785.

[104] K. O. Christe, W. Sawodny, J. P. Guertin, *Inorg. Chem.* **1967**, *6*, 1159.

[105] T. Surles, L. A. Quarterman, H. H. Hyman, *J. Inorg. Nucl. Chem.* **1973**, *35*, 668.

[106] D. Naumann, A. Meurer, *J. Fluor. Chem.* **1995**, *70*, 83.

[107] X. Zhang, K. Seppelt, *Z. Anorg. Allg. Chem.* **1997**, *623*, 491.

[108] K. O. Christe, W. W. Wilson, G. W. Drake, M. A. Petrie, J. A. Boatz, *J. Fluor. Chem.* **1998**, *88*, 185.

[109] R. Minkwitz, R. Bröchler, R. Ludwig, *Inorg. Chem.* **1997**, *36*, 4280.

[110] Y. Ogawa, O. Takahashi, O. Kikuchi, *J. Mol. Struct.* **1998**, *429*, 187.

[111] K. S. Thanthiriwatte, M. Vasiliu, D. A. Dixon, K. O. Christe, *Inorg. Chem.* **2012**, *51*, 10966.

[112] J. H. Miller, L. Andrews, *Inorg. Chem.* **1979**, *18*, 988.

[113] R. D. Hunt, C. Thompson, P. Hassanzadeh, L. Andrews, *Inorg. Chem.* **1994**, *33*, 388.

[114] A. Walsh, *J. Chem. Soc.* **1953**, 2266.

[115] W. Schnick, M. Jansen, *Angew. Chem. Int. Ed.* **1985**, *24*, 54; W. Schnick, M. Jansen, *Angew. Chem.* **1985**, *97*, 48.

[116] W. Hesse, M. Jansen, W. Schnick, *Prog. Solid St. Chem.* **1989**, *19*, 47.

[117] W. Kutzelnigg, *Angew. Chem. Int. Ed.* **1984**, *23*, 272; W. Kutzelnigg, *Angew. Chem.* **1984**, *96*, 262.

[118] A. Pargellis, *J. Chem. Phys.* **1990**, *93*, 2099.

[119] J. Szczepanski, S. Ekern, M. Vala, *J. Phys. Chem. A* **1997**, *101*, 1841.

[120] J. Szczepanski, C. Wehlburg, M. Vala, *J. Phys. Chem. A* **1997**, *101*, 7039.

[121] K. Raghavachari, *Z. Phys. D* **1989**, *12*, 61.

[122] K. Raghavachari, *Chem. Phys. Lett.* **1990**, *171*, 249.

[123] J. D. Watts, R. J. Bartlett, *J. Chem. Phys.* **1992**, *97*, 3445.

[124] M. Giuffreda, M. Deleuze, J.-P. François, *J. Phys. Chem. A* **2002**, *106*, 8569.

[125] H. Wang, G. Li, *Eur. Phys. J. D* **2014**, *68*, 182.

[126] M. Polak, M. Gruebele, R. J. Saykally, *J. Am. Chem. Soc.* **1987**, *109*, 2884.

[127] M. Polak, M. Gruebele, G. S. Peng, R. J. Saykally, *J. Chem. Phys.* **1988**, *89*, 110.

[128] C. Brazier, P. Bernath, J. B. Burkholder, C. J. Howard, *J. Chem. Phys.* **1988**, *89*, 1762.

[129] C. Brazier, P. Bernath, *J. Chem. Phys.* **1988**, *88*, 2112.

[130] R. Tian, J. C. Facelli, J. Michl, *J. Phys. Chem.* **1988**, *92*, 4073.

[131] R. Tian, V. Balaji, J. Michl, *J. Am. Chem. Soc.* **1988**, *110*, 7225.

[132] G. V. Chertihin, L. Andrews, M. Neurock, *J. Phys. Chem.* **1996**, *100*, 14609.

[133] L. Andrews, W. D. Bare, G. V. Chertihin, *J. Phys. Chem. A* **1997**, *101*, 8417.

[134] L. Andrews, A. Citra, G. V. Chertihin, W. D. Bare, M. Neurock, *J. Phys. Chem. A* **1998**, *102*, 2561.

[135] G. V. Chertihin, L. Andrews, C. W. Bauschlicher, *J. Am. Chem. Soc.* **1998**, *120*, 3205.

[136] G. V. Chertihin, W. D. Bare, L. Andrews, *J. Phys. Chem. A* **1998**, *102*, 3697.

[137] M. Zhou, L. Andrews, *J. Phys. Chem. A* **1998**, *102*, 9061.

[138] S. P. Willson, L. Andrews, *J. Phys. Chem. A* **1998**, *102*, 10238.

[139] S. P. Willson, L. Andrews, *J. Phys. Chem. A* **1999**, *103*, 1311.

[140] A. Citra, L. Andrews, *J. Phys. Chem. A* **1999**, *103*, 3410.

[141] L. Andrews, P. F. Souter, W. D. Bare, B. Liang, *J. Phys. Chem. A* **1999**, *103*, 4649.

[142] M. Zhou, L. Andrews, *J. Phys. Chem. A* **2000**, *104*, 1648.

[143] L. Andrews, M. Zhou, G. V. Chertihin, W. D. Bare, Y. Hannachi, *J. Phys. Chem. A* **2000**, *104*, 1656.

[144] A. Citra, L. Andrews, *J. Phys. Chem. A* **2000**, *104*, 1152.

[145] K. Sankaran, K. Sundararajan, K. Viswanathan, *J. Phys. Chem. A* **2001**, *105*, 3995.

[146] A. Citra, X. Wang, W. D. Bare, L. Andrews, *J. Phys. Chem. A* **2001**, *105*, 7799.

[147] X. Wang, L. Andrews, *J. Phys. Chem. A* **2002**, *106*, 2457.

[148] B. Vlaisavljevich, L. Andrews, X. Wang, Y. Gong, G. P. Kushto, B. E. Bursten, *J. Am. Chem. Soc.* **2016**, *138*, 893.

[149] P. Sebald, C. Stein, R. Oswald, P. Botschwina, *J. Phys. Chem. A* **2013**, *117*, 13806.

[150] A. Langseth, J. R. Nielsen, J. U. Sørensen, *Z. Phys. Chem.* **1934**, *27*, 100.

[151] P. Gray, T. Waddington, *Trans. Faraday Soc.* **1957**, *53*, 901.

[152] R. Dreyfus, P. Levy, *Proc. Royal Soc.* **1958**, *246*, 233.

[153] H. A. Papazian, *J. Chem. Phys.* **1961**, *34*, 1614.

[154] J. I. Bryant, *J. Chem. Phys.* **1963**, *38*, 2845.

[155] J. I. Bryant, *J. Chem. Phys.* **1964**, *40*, 3195.

[156] J. I. Bryant, *J. Chem. Phys.* **1966**, *45*, 689.

[157] M. Baudler, G. Brauer, F. Feher, F. Huber, R. Klement, W. Kwasnik, P. W. Schenk, M. Schmeisser, R. Steudel, *Handbuch der präparativen anorganischen Chemie*, *Vol. 1*, 3rd ed., (Ed.: G. Brauer), Ferdinand Enke Verlag, **1975**, p. 458.

[158] P. Cosby, J. Moseley, J. Peterson, J. Ling, *J. Chem. Phys.* **1978**, *69*, 2771.

[159] S. E. Novick, P. C. Engelking, P. L. Jones, J. H. Futrell, W. Lineberger), *J. Chem. Phys.* **1979**, *70*, 2652.

[160] J. Hiller, M. Vestal, *J. Chem. Phys.* **1981**, *74*, 6096.

[161] L. Wang, S. Woo, E. Helmy, *Phys. Rev. A* **1987**, *35*, 759.

[162] D. W. Arnold, C. Xu, E. H. Kim, D. M. Neumark, *J. Chem. Phys.* **1994**, *101*, 912.

[163] J. C. Bopp, A. N. Alexandrova, B. M. Elliott, T. Herden, M. A. Johnson, *Int. J. Mass Spectrom.* **2009**, *283*, 94.

[164] B. B. Shen, Y. Benitez, K. G. Lunny, R. E. Continetti, *J. Chem. Phys.* **2017**, *147*, 094307.

[165] W. Klein, K. Armbruster, M. Jansen, *Chem. Commun.* **1998**, 707.

[166] T. Kellersohn, N. Korber, M. Jansen, *J. Am. Chem. Soc.* **1993**, *115*, 11254.

[167] M. E. Jacox, D. E. Milligan, *J. Mol. Spec.* **1972**, *43*, 148.

[168] M. Jacox, D. Milligan, *Chem. Phys. Lett.* **1972**, *14*, 518.

[169] L. Andrews, *J. Am. Chem. Soc.* **1973**, *95*, 4487.

[170] L. Andrews, R. C. Spiker Jr, *J. Chem. Phys.* **1973**, *59*, 1863.

[171] R. C. Spiker Jr, L. Andrews, *J. Chem. Phys.* **1973**, *59*, 1851.

[172] L. Andrews, B. S. Ault, J. M. Grzybowski, R. O. Allen, *J. Chem. Phys.* **1975**, *62*, 2461.

[173] C. L. Lugez, W. E. Thompson, M. E. Jacox, *J. Chem. Phys.* **1996**, *105*, 2153.

[174] K. A. Peterson, R. C. Mayrhofer, R. C. Woods, *J. Chem. Phys.* **1990**, *93*, 5020.

[175] W. Koch, G. Frenking, G. Steffen, D. Reinen, M. Jansen, W. Assenmacher, *J. Chem. Phys.* **1993**, *99*, 1271.

[176] P. Borowski, B. O. Roos, S. C. Racine, T. J. Lee, S. Carter, *J. Chem. Phys.* **1995**, *103*, 266.

[177] T. J. Lee, C. E. Dateo, M. Rubio, B. O. Roos, *Collect. Czech. Chem. Commun.* **2003**, *68*, 189.

[178] E. P. Lee, T. G. Wright, *J. Phys. Chem. A* **2004**, *108*, 4792.

[179] E. P. Lee, T. G. Wright, *Chem. Phys. Lett.* **2005**, *403*, 119.

[180] H. Moissan, *Compt. Rend.* **1889**, *109*, 809.

[181] A. Sharpe, *J. Chem. Soc.* **1949**, 2901.

[182] L. Asprey, F. Kruse, K. Jack, R. Maitland, *Inorg. Chem.* **1964**, *3*, 602.

[183] F. Einstein, P. Rao, J. Trotter, N. Bartlett, *J. Chem. Soc. A* **1967**, 478.

[184] M. Dove, P. Benkič, C. Platte, T. Richardson, N. Bartlett, *J. Fluor. Chem.* **2001**, *110*, 83.

[185] X. Wang, L. Andrews, K. Willmann, F. Brosi, S. Riedel, *Angew. Chem. Int. Ed.* **2012**, *51*, 10628; X. Wang, L. Andrews, K. Willmann, F. Brosi, S. Riedel, *Angew. Chem.* **2012**, *124*, 10780.

[186] X. Wang, L. Andrews, F. Brosi, S. Riedel, *Chem. Eur. J.* **2013**, *19*, 1397.

[187] D. Schröder, J. Hrušák, I. C. Tornieporth-Oetting, T. M. Klapötke, H. Schwarz, *Angew. Chem. Int. Ed.* **1994**, *33*, 212; D. Schröder, J. Hrušák, I. C. Tornieporth-Oetting, T. M. Klapötke, H. Schwarz, *Angew. Chem.* **1994**, *106*, 223.

[188] C. J. Evans, M. C. Gerry, *J. Am. Chem. Soc.* **2000**, *122*, 1560.

[189] P. Schwerdtfeger, P. D. Boyd, A. K. Burrell, W. T. Robinson, M. J. Taylor, *Inorg. Chem.* **1990**, *29*, 3593.

[190] A. Pérez-Bitrián, M. Baya, J. M. Casas, A. Martín, B. Menjón, J. Orduna, *Angew. Chem. Int. Ed.* **2018**, *57*, 6517; A. Pérez-Bitrián, M. Baya, J. M. Casas, A. Martín, B. Menjón, J. Orduna, *Angew. Chem.* **2018**, *130*, 6627.

[191] M. A. Ellwanger, PhD thesis, Freie Universität Berlin, **2019**.

[192] R. Hoppe, W. Klemm, *Z. Anorg. Allg. Chem.* **1952**, *268*, 364.

[193] R. Hoppe, R. Homann, *Z. Anorg. Allg. Chem.* **1970**, *379*, 193.

[194] G. Lucier, L. Elder, S.H.and Chacón, N. Bartlett, *Eur. J. Solid State Inorg. Chem.* **1996**, *33*, 809.

[195] R. Schmidt, B. Müller, *Z. Anorg. Allg. Chem.* **2004**, *630*, 2393.

[196] K. Leary, N. Bartlett, *J. Chem. Soc. Chem. Commun.* **1972**, 903.

[197] M. A. Ellwanger, S. Steinhauer, P. Golz, H. Beckers, A. Wiesner, B. Braun-Cula, T. Braun, S. Riedel, *Chem. Eur. J.* **2017**, *23*, 13501.

[198] I.-C. Hwang, K. Seppelt, *Angew. Chem. Int. Ed.* **2001**, *40*, 3690; I.-C. Hwang, K. Seppelt, *Angew. Chem.* **2001**, *113*, 3803.

[199] D. Himmel, S. Riedel, *Inorg. Chem.* **2007**, *46*, 5338.

[200] A. Timakov, V. Prusakov, I. Drobyshevskii, *Dokl. Akad. Nauk SSSR* **1986**, *291*, 125.

# 7 List of Publications

## Articles


[1] **Frenio A. Redeker**, Helmut Beckers and Sebastian Riedel, IR Laser-Ablation of KCN: A Surprisingly Simple Route to Polynitrogen and Polycarbon Species, **2019**, *Chem. Eur. J.* **2019**, accepted.
https://doi.org/10.1002/chem.201905103

[2] **Frenio A. Redeker**, Mathias A. Ellwanger, Helmut Beckers and Sebastian Riedel, Investigation of Molecular Alkali Tetrafluorido Aurates by Matrix-Isolation Spectroscopy, *Chem. Eur. J.* **2019**, *25*, 15059–15061.
https://doi.org/10.1002/chem.201904335

[3] Karsten Sonnenberg, Lisa Mann, **Frenio A. Redeker**, Benjamin Schmidt and Sebastian Riedel, Poly and Interhalogen Anions from Fluorine to Iodine, *Angew. Chem. Int. Ed.* **2019**, accepted.
https://doi.org/10.1002/anie.201903197

[4] Stefan Mattsson, Beate Paulus, **Frenio A. Redeker**, Helmut Beckers, Sebastian Riedel, and Carsten Müller, The Crystal Structure of $\alpha$-$F_2$: Solving a 50 Year Old Puzzle Computationally, *Chem. Eur. J.* **2019**, *25*, 3318–3324.
https://doi.org/10.1002/chem.201805300

[5] **Frenio A. Redeker**, Alexey Kropman, Carsten Müller, Sarah E. Zewge, Helmut Beckers, Beate Paulus and Sebastian Riedel, Theoretical Investigation of the Structures, Stabilities and Vibrational Properties of Triatomic Interhalide Ions and their Alkali Ion Pairs, *J. Fluor. Chem.* **2018**, *216*, 81-88.
https://doi.org/10.1016/j.jfluchem.2018.10.007

[6] **Frenio A. Redeker**, Helmut Beckers and Sebastian Riedel, Matrix-Isolation and Comparative Far-IR Investigation of Free Linear $[Cl_3]^-$ and a Series of Alkali Trichlorides, *Chem. Commun.* **2017**, *53*, 12958–12961.
https://doi.org/10.1039/c7cc08290h

[7] **Frenio A. Redeker**, Helmut Beckers and Sebastian Riedel, Investigation of Alkali Metal Polyfluorides by Matrix-Isolation Spectroscopy, *RSC Adv.* **2015**, *5*, 106568–106573.
https://doi.org/10.1039/c5ra24227d

## Conference Contributions – Oral Presentations

[1] **Frenio A. Redeker**, Helmut Beckers and Sebastian Riedel, Matrix-Isolation of Free Polyhalide Anions and Alkali Trihalides by Laser Ablation of Salts, *Chemistry and Physics at Low Temperatures* **2018**, Laramie, USA.

## Conference Contributions – Poster Presentations

[1] **Frenio A. Redeker**, Helmut Beckers and Sebastian Riedel, Polyhalide Anions – Isolated in Noble Gas Matrices, *Chemistry and Physics at Low Temperatures* **2018**, Laramie, USA.

[2] **Frenio A. Redeker**, Helmut Beckers and Sebastian Riedel, Polyhalide Anions – Isolated in Noble Gas Matrices, *GDCh Wissenschaftsforum Chemie* **2017**, Berlin, Germany.

[3] **Frenio A. Redeker**, Helmut Beckers, Stefanie Kieninger and Sebastian Riedel, Laser Ablation of Metal Halides, *18. Vortragstagung der Wöhler-Vereinigung* **2016**, Berlin, Germany.